ELSEVIER

Food Chemistry 82 (2003) 3–22

Food Chemistry

www.elsevier.com/locate/foodchem

Cluster composition of liquid water derived from laser-Raman spectra and molecular simulation data

Maciej Starzak[a,*], Mohamed Mathlouthi[b]

[a]*School of Chemical Engineering, University of Natal, 4041 Durban, South Africa*

[b]*Laboratoire de Chimie Physique Industrielle, Université de Reims Champagne-Ardenne, 51687 Reims Cédex, France*

Abstract

Studying the behaviour of aqueous solutions of carbohydrates and other molecules commonly encountered in food science always leads to the fundamental question about the structure of bulk liquid water. The present study is an attempt towards the development of a mixture model of water structure based on information derived from experimental Raman spectra of water as well as molecular simulation data of isolated water clusters. The model assumes that liquid water is a thermodynamically ideal mixture of small water clusters in a state of chemical equilibrium. The equilibrium obeys the law of mass action and the van't Hoff temperature dependence of equilibrium constants. In order to validate the model and estimate its chemical equilibrium constants, Raman spectra of liquid water, predicted by the model, were compared with the isotropic components of carefully selected experimental spectra of pure liquid water, determined in the stretching vibration region at various temperatures. The theoretical Raman spectrum of bulk water was obtained by superposition of spectra of individual clusters, assuming their composition-based additivity. The spectra of small clusters were obtained from the Gaussian 98 programme using the 6-311+G(d,p) basis set together with the BLYP method. The model can reproduce the main features of the experimental Raman spectra of liquid water in the entire range of stretching vibration frequencies, at temperatures ranging from −30 to 300 °C. The resulting cluster composition of liquid water was found to be strongly temperature-dependent. At room temperature, water tetramer and pentamer are predominant, whereas the predicted concentrations of monomeric and dimeric water are very low. The latter gradually increase with increasing temperature at the expense of larger clusters. At its current stage of development, the model should be considered an alternative mathematical tool for more rational and rigorous analysis and interpretation of the Raman spectra of liquid water rather than a definite model of bulk water structure.

Keywords: Water; Liquid structure; Cluster; Molecular association; Hydrogen bond; Raman spectra

1. Introduction

As the most ubiquitous chemical compound on the Earth's surface, water has probably received more scientific and technological attention than any other substance. Much of this interest is due to the role that liquid water plays in physical chemistry of condensed phases, reaction chemistry (strong solvent effects on reactions), biochemistry and biology (water-protein interactions, effect on microbial growth), atmospheric science (formation of clouds and acid rain), as well as more practically orientated disciplines, such as food science (effect of water activity on food quality and preservation) or sugar technology (drying and conditioning of sugar crystals).

In contrary to other liquids, water and aqueous solutions exhibit in many respects unique ("anomalous") thermodynamic and transport properties which strongly depend on temperature and pressure. The well-known anomalies of pure liquid water include: a negative volume of melting, density maximum at 4 °C, isothermal compressibility minimum at 46 °C, very high melting, boiling and critical temperature, high heat of vaporization, high constant-pressure heat capacity, high dielectric constant, and decreasing viscosity with increasing pressure. The existence of many of these unusual properties is believed to be due to the hydrogen bonding prevalent in water as well as its cooperativity. As bulk properties are the manifestation of molecular

* Corresponding author. Fax: +27-031-260-1118.
E-mail address: starzak@nu.ac.za (M. Starzak).

0308-8146/03/$ - see front matter
doi:10.1016/S0308-8146(02)00584-8

Nomenclature

c	coefficient of polynomial, Eq. (5)
E_0	total electronic energy per cluster molecule
h	Planck constant
H	sum of electronic and thermal enthalpy per cluster molecule
I	Raman intensity
k	Boltzmann constant
K_A	clustering equilibrium constant
L	local field correction to Raman intensity
n	refractive index
N	number of scattering molecules
r	O–H bond length in water monomer
R	universal gas constant
S	isotropic Raman scattering activity
T	absolute temperature
w	intensity peak width at half maximum
x	cluster-based mole fraction
α'	isotropic part of the symmetric polarizability tensor
γ'	anisotropic part of the symmetric polarizability tensor
ΔH_A	incremental molar enthalpy of water clustering
ζ	frequency scaling factor
θ	H–O–H angle in water monomer
ν	vibrational frequency
ρ	depolarization ratio

interactions, a full understanding of water behaviour requires consideration at the molecular level. Hence, the geometry and the charge distribution of the isolated water molecule are of fundamental importance. In a simple four-point-charge representation (Bjerrum, 1952), the water molecule is depicted as a quadrupole with two protons and two lone electron pairs at the corners of a tetrahedron with oxygen in its centre. Such a geometry and charge distribution favour the formation of a hydrogen-bonded network or agglomeration of water molecules with four O–H–O bonds per molecule, where the water molecules act as hydrogen bond donors and acceptors. In addition, the slight covalency of a hydrogen bond modifies the charge distribution on water molecules in such a way that the hydrogen-bonded molecules are more likely to form additional hydrogen bonds than unbonded molecules, leading to a phenomenon known as hydrogen bond cooperativity (Frank & Wen, 1957). Hydrogen bonding also exists in other liquids such as alcohols. But as there is only one hydroxyl group per molecule of alcohol, the molecules form chains or rings rather than a three-dimensional tetrahedral network. The structure of hexagonal ice Ih, isomorphous with the tridymite structure of silica, is an ideal representation of this three-dimensional network. In the liquid state, however, the long-range order cannot be maintained and, as has been demonstrated in numerous X-ray and neutron scattering studies, only short-range positional and orientational correlations are approximately retained. Another difference from solid ice is that hydrogen bonds are distorted and arranged irregularly after melting. Moreover, due to thermal reorientation, the lifetime of a given molecular ordering is extremely short, locally rearranging on a picosecond scale. Apparently, a temperature-dependent competition exists between the ordering effects of hydrogen bonding and the disordering kinetic effects. With increasing temperature, the time-averaged hydrogen-bonded network gradually breaks down and, as a result, water loses its unique properties. Some degree of hydrogen bonding, however, is still retained, even at the critical point of water.

2. Structural models of bulk water

Historically, there are two competing and, to some extent, complementary theoretical approaches used to describe the molecular structure of liquid water. In general, they are represented by the continuum (uniform) models and the mixture (cluster) models. Both categories make use of some experimental properties of water and a great deal of intuition. Unfortunately, of the countless models put forward, over more than a century, none can adequately fit both the physical properties and the available structural data.

In continuum models, the hydrogen bonding is assumed to be almost complete. Consequently, water is thought to exist as a continuous network of molecules interconnected by somewhat distorted hydrogen bonds. The existence of qualitatively different kinds of molecules is entirely negated in these models and the whole water sample is viewed as a single entity with temperature-dependent local structure. All the structural parameters of hydrogen bonding (distances and angles), as well as bond energies, are continuously distributed. The corresponding partition functions contain several parameters, which have to be adjusted to fit a range of experimental properties. The essential characteristics of all continuum models originate from the pioneering work of Bernal and Fowler (1933). The distorted tetrahedral network model of Pople (1951), closely related random network models of Bernal (1964) and Angell (1971), and much more advanced, the so-called Sceats–Rice random network model (RNM) (Sceats, Stavola, & Rice, 1979), are classic examples in this category. The continuum models are incompatible with the thermodynamic anomalies of water such as the density maximum and compressibility minimum. They also cannot account for the remarkable effect of temperature on the intensity distribution in the stretching vibration region of the Raman spectra of liquid water.

Generally speaking, mixture models describe liquid water as an equilibrium mixture of species which are distinguishable in an instantaneous picture. For many years they have been used to explain the properties of water and aqueous solutions. Contrary to the continuum models, the mixture models have been proposed with more variety. Most mixture models assume that water molecules exist in a few (often two) classes of more or less well-defined structural entities. However, as properly stressed by Nemethy (1974), the term "mixture" has often been used in different contexts. Sometimes it implies only that a hydrogen-bond forming and breaking equilibrium is considered, and the existence of distinct molecular species is not explicitly assumed. Therefore, one should differentiate between mixture models of certain species and mixture models which discuss H-bonded and non-H-bonded OH groups.

Modern history of mixture models starts with a paper by Röntgen (1892), which describes water as a saturated solution of ice in a liquid composed of simpler molecules. Later, Sutherland (1900) proposed a three-component model and assigned the names hydrol, dihydrol and trihydrol to H_2O, $(H_2O)_2$ and $(H_2O)_3$, respectively. Over the next 50 years a number of simple mixture models were proposed, based on a coupled equilibrium of small water aggregates (see Dorsey, 1940), amongst which the associate model of Eucken (1946, 1949), involving the formation of $(H_2O)_n$, with $n = 1,2,4,8$, was perhaps more successful than others in predicting selected physical properties of water. For the following three decades, the mixture models gradually evolved towards systems composed of large, not necessarily regular, clusters. A variety of structural arrangements have been proposed for these entities, varying from isomorphs of ice to clathrate types. Some models, as for example the flickering cluster model (Frank & Quist, 1961; Frank & Wen, 1957), allowed for a variation in the type, size or number of the short-lived structural units, caused by either a temperature or pressure change.

The first attempt to apply statistical thermodynamics to mixture models was made by Némethy and Scheraga (1962). They postulated the presence of a distribution of hydrogen-bonded clusters within the liquid. The model predicts only negligible quantities of either monomers or very large clusters (>60). The mean cluster size changes with temperature to give smaller clusters at high temperatures. At 0 °C, it was found to be about 11 (Hagler, Scheraga, & Némethy, 1972). A revised version of this model was proposed by Lentz, Hagler, and Scheraga (1974), who assumed that liquid water is composed of a finite number of small clusters (from monomer to nonamer). According to this model, pentamer and hexamer are the most abundant forms of water between 0 and 100 °C (on H_2O basis). A similar approach applied to a hypothetical system involving two solid-like clusters (46 molecule ice-I-like and 46 molecule ice-III-like) in equilibrium with each other and with monomer water, was proved to be successful in predicting most of thermodynamic properties of water (Jhon, Grosh, Ree, & Eyring, 1966). However, a large number of adjustable parameters made this model highly empirical.

In the early 1960s the high resolution Raman technique became available and the spectral band shapes have since been carefully analysed in an effort to find evidence for the mixture theory. The spectroscopic model of Walrafen (1967), involving nonhydrogen-bonded monomeric water and lattice water, and a similar two-component model of Libnau, Toft, Christy, and Kvalheim (1994) are here prominent examples. According to Walrafen, Fisher, Hokmabadi, and Yang (1986), the experimentally demonstrated existence of isosbestic points in both the isotropic and anisotropic Raman spectra of liquid water (Hare & Sorensen, 1990; Walrafen, Hokmabadi, & Yang, 1986) constitutes strong evidence for a mixture model of water involving at least two different structural components. In several other spectroscopic studies, the Raman spectra were also interpreted in favour of the mixture models (Durig, Gounev, Nashed, Ravindranath, Srinivas, & Rao, 1999; Luu, Luu, Rull, & Sopron, 1982; Rao & Ramanaiah, 1966).

With the advent of supercomputers more rigorous quantitative studies on water structure could be performed based on quantum and statistical mechanics. Various molecular interaction potentials for the water molecule (fitted either to results of ab initio calculations or to empirical data) have been used, together with powerful computational techniques, such as the Monte Carlo or Molecular Dynamics method. The first computer "experiment" of this type was carried out by Rahman and Stillinger (1971) with a model of 216 water molecules applying the effective pair potential of Ben-Naim and Stillinger (1972). This study can be regarded as a turning point in the theoretical approach. Since that time, the need for classic continuum and mixture models has been overcome by the possibility of performing more rigorous analyses via the molecular simulation techniques. A number of new models have been published over the past two decades, in which more and more complicated structural units were suggested as the building blocks for liquid water, including aggregates of water in ice-like arrangements discussed by Luck (1976), a network of hexagonal, pentagonal and dodecahedral arrays (Dougherty & Howard, 1998) or a fluctuating arrangement of 14-molecule tetrahedral units, leading to the formation of three-nanometer 280-molecule expanded icosahedral clusters (Chaplin, 1999), to mention just a few more recent proposals. Naturally, with the growing size of basic structural units believed to constitute liquid water, the fundamental differences between mixture and continuum theories have become meaningless and are now semantic rather than based on physical arguments.

Despite enormous effort and great progress in liquid-state theory of water, none of the models mentioned earlier has been fully accepted by the scientific community and recognized as the complete and satisfactory representation of liquid water over a wide range of temperatures and pressures. According to many authors, the difficulty in obtaining a rigorous molecular-scale description of water structure is largely a consequence of the extended, dynamic hydrogen-bonded network that exists throughout the liquid, whereas the most popular effective (empirical) water intermolecular potentials used to simulate liquid water behaviour are explicitly pairwise (water–water) additive. They include the crucial effects of cooperativity only implicitly, through the potential parameters rather than many-body interaction terms. The many-body terms are believed to play an important role in bulk properties of water. For example, in the water hexamer, many-body forces contribute about 1/5 of the total binding energy of the cluster (Xantheas, 1994). In addition, most of the empirical water potentials do not account for the polarizability of individual molecules and ignore the fact that the water molecule is itself flexible and distortable (Liu, Brown, Carter, Saykally, Gregory, & Clary, 1996a; Liu, Cruzan, & Saykally, 1996b).

Rigorous mixture models derived from intermolecular potentials, even if successful in predicting selected physical properties of bulk water (including its well-known anomalies), are computationally very expensive. This limits their practical usefulness, especially when applied to engineering-related problems. The need for prediction of water activity, encountered in many areas of food science and sugar technology, is a good example here. Early mixture models involving small water clusters are particularly attractive if one wants to study water activity in aqueous solutions by adopting the formalism of chemical thermodynamics and treating the solution as a reactive system in a state of chemical equilibrium. In an attempt to revitalise the simple mixture models of liquid water, Benson and Siebert (1992) studied equilibrium isomerization between polar cyclic tetramers and low-symmetry cubic octamers. Their semi-empirical model, with a firm thermodynamic foundation, reproduces the anomalous heat capacity of liquid water from 0 to 100 °C within $\pm 2\%$ error. According to the same authors, monocyclic pentamers and polycyclic decamers may also exist in liquid water and play a similar role.

3. Small water clusters

The past 10–15 years has brought a real flood of computer simulation studies on fundamental properties of isolated small clusters of water, including their geometry, energetics, thermochemistry, and vibrational (infrared and Raman) spectra. Recent progress in laser spectroscopy experiments (e.g. the jet-cooled direct absorption spectroscopy in the microwave, terahertz, and infrared regions of the spectrum) has also facilitated new, highly detailed studies of water clusters. Since the water trimer, tetramer, pentamer and hexamer are some of the dominant structures identified in room-temperature liquid water (Belch & Rice, 1987; Luu et al., 1982; Speedy, Madura, & Jorgensen, 1987), it is believed that these studies will provide a means of quantifying the intermolecular forces and hydrogen-bond rearrangements that occur in condensed phases, for the ultimate development of an accurate many-body water potential.

The isolated water cluster is understood as a fixed number of water molecules placed in a three-dimensional space in an energetically favourable mutual orientation. Two water molecules constituting a dimer can exhibit at least four different optimal geometries (*trans*-linear, open-chain, planar-ring and bifurcated) at which their interaction potential passes through a local minimum (Wicke, 1966). However, since these four conformers have different binding as well as Gibbs free energies, they are not equally favourable (stable). In the case of water dimer, the *trans*-linear geometry was experimentally found to be most stable (Dyke, Mack, & Muenter, 1977) and correspond to the global minimum of potential energy (Honegger & Leutwyler, 1988). Unfortunately, with the increasing cluster size, the number of all possible conformers increases dramatically. Furthermore, the same global minimum structure exists in a number of ‘‘versions’’, differing only by permutations of identical atoms that do not break chemical bonds (Liu, Cruzan et al., 1996). This makes the search for the most favourable structure an extremely tedious computational task. In fact, getting a definite answer is even more difficult since the differences between energy levels of individual conformers are often very small (<0.5 kcal/mol) whilst the results of molecular simulation are sensitive to the employed method of calculation (such as the type of the empirical potential assumed or the size of basis set and the level of theory in ab initio calculations). However, due to their different geometries, energetically similar conformers may exhibit quite different rotational and vibrational dynamics. The experimental determination of these dynamic properties, by using terahertz (far-infrared) laser vibration–rotation tunnelling spectroscopy, provides useful criteria for cluster structure discrimination. The most recent experimental and theoretical studies strongly suggest that the water trimer, tetramer and pentamer have quasi-planar cyclic minimum energy structures. Although the hexamer has been a subject of controversy for some time, a three-dimensional cage-like structure is probably its most stable form (Liu, Brown et al., 1996).

Larger clusters are expected to have three-dimensional geometries.

Vibrational spectra of small water clusters have also been extensively studied theoretically over the past decade. Honegger and Leutwyler (1988) and Knochenmuss and Leutwyler (1992) used the ab initio molecular orbital method at the SCF level with the 4-31G basis set to predict, in the harmonic approximation level, the vibrational frequencies of $(H_2O)_{n=2–5,8}$, together with the corresponding infrared and Raman peak intensities. In a series of similar studies, Burke and co-workers (Burke, Jensen, Jensen, & Krishnan, 1993; Jensen, Krishnan, & Burke, 1995a, 1995b, 1996; Krishnan, Jensen, & Burke, 1994) determined vibrational spectra of various clusters ($n = 5–9$) using the Hartree–Fock (HF) method with 6-311G(d) and 6-311G(d,p) basis sets. Selected frequency data obtained at various levels of theory (MP2, MP3, MP4, BLYP, B3LYP, BVWN and others) can be found in studies by Kim and Kim (1998; Kim, Lee, Lee, Mhin & Kim, 1995; Kim, Majumdar, Lee, & Kim, 1999; Kim, Mhin, Choi, & Lee; 1992), Xantheas (1995) and Xantheas and Dunning (1993).

4. A chemical cluster model of liquid water

4.1. Hypothetical mechanism of water clustering

Symons (1972) presented interesting arguments in favour of the "mixture of clusters" model of liquid water. Essentially, they were all derived from the double bifunctional acid-base behaviour of the water molecule, coupled with its near-tetrahedral directional geometry. Symons considers water initially dissolved in a hypothetical inert solvent. At very low concentrations, water is dissolved in the monomeric state, each molecule having two acid and two base functions. With increasing concentration, as water monomers begin to polymerize, dimers will first be formed with three acids and three basic sites available for further association. Therefore, there will be a higher probability of a monomer interacting with a dimer than with another monomer. Since the addition of each molecule produces two new suitable sites of attachment to the cluster, eventually, the total amount of water would be transformed into a giant polymer. However, this will not take place, since the new vacant connection sites are not equally reactive. Their reactivity depends on their location within the existing cluster. In the dimer molecule, for example, the oxygen atom involved in the hydrogen bond becomes less reactive than the other oxygen. Analogously, the two positively charged hydrogen atoms are more reactive than the third available hydrogen. The distribution of site reactivities becomes more complicated for larger clusters, especially with the increasing probability of chain branching, cyclization and formation of three-dimensional structures. Symons (1972) formulated a set of rules allowing for a rough comparative estimation of these reactivities. The chief conclusions of his analysis appear to render improbable all those models involving the coexistence of ice-like units and monomeric water. They also rule out concepts admitting cooperative rapid breakdown or building up of structural units as, for example, in the theory of flickering clusters. Instead, his arguments speak in favour of a model in which liquid water is a mixture of relatively small clusters, which are subject to certain limited transformations involving both the formation and break-up of hydrogen bonds. A thermodynamic chemical equilibrium model seems to be the simplest way to describe this situation.

The recent progress in molecular modelling of small water clusters, as well as high quality laser-Raman spectroscopic measurements of liquid water, now available over a wide range of temperatures, allow for developing a simple cluster model of liquid water which would satisfy the conditions of chemical equilibrium. Such a model, due to its simplicity, can be easily extended to systems involving non-ionic water-soluble substances, and can finally be used to predict water activity in the aqueous solution.

4.2. Basic model assumptions

The proposed model considers bulk liquid water as a mixture of small water clusters (including water monomer), with decamer being the largest possible cluster ($n = 10$). Although such a choice is rather arbitrary, several previous modelling attempts, involving small clusters (Arakawa, Tokiwano, & Kojima, 1977; Benson & Siebert, 1992; Eucken, 1946, 1949; Hagler et al., 1972; Lentz et al., 1974), resulted in a similar size range. The clusters remain in a state of chemical equilibrium, being constantly subjected to the following instantaneous association-dissociation processes (reversible clustering reactions):

$$(H_2O)_{i-1} + H_2O \xleftrightarrow{K_{A,i-1}} (H_2O)_i, \quad i = 2, \ldots, \quad n \tag{1}$$

It should be noted that the reaction network defined by Eq. (1) is not the only theoretically possible scheme which can yield the required variety of water clusters. One can easily imagine different modes of association resulting in the same products (e.g. formation of a cube octamer from two cyclic tetramers). It can be easily shown, however, that they are linear combinations of the reactions adopted earlier and, consequently, will produce the same equilibrium composition of a mixture of clusters.

The proposed chemical equilibria are temperature-dependent and the classic van't Hoff formalism applies with two constant parameters per clustering reaction, i.e. the chemical equilibrium constant K°_{Ai} at temperature $T_{\circ}$

and the temperature-independent enthalpy of clustering (association) ΔH_{Ai}:

$$K_{Ai} = K^{\circ}_{Ai}\exp\left[\frac{\Delta H_{Ai}}{R}\left(\frac{1}{T_{\circ}} - \frac{1}{T}\right)\right], \quad i = 1, \; 2, \ldots, \; n-1 \tag{2}$$

The mixture of water clusters is assumed to be thermodynamically non-ideal. However, all physical interactions are ignored, and the non-ideality results exclusively from the presence of chemical (clustering) reactions. In such an "ideal" associated mixture, the activities of individual clusters are equal to their equilibrium mole fractions in solution (Prigogine & Defay, 1954). In the state of chemical equilibrium, the Gibbs free energy attains a minimum. Since for the ideal associated mixtures, the Gibbs free energy becomes a function of composition rather than thermodynamic activities, the resulting mass action law can be written in terms of mole fractions as well:

$$K_{Ai} = \frac{\left[(\mathrm{H_2O})_{i+1}\right]}{\left[(\mathrm{H_2O})_i\right]\,[\mathrm{H_2O}]} = \frac{x_{i+1}}{x_i x_1}, \quad i = 1, \; 2, \; \ldots, \; n-1 \tag{3}$$

where x_i is the mole fraction of ith cluster. It has to be emphasized that the mole fractions used in the chemical equilibria are cluster-based rather than based on the monomeric water content. Given the equilibrium parameters of the earlier model, the cluster composition of liquid water can be predicted at any temperature by solving the system of algebraic Eq. (3) and the condition:

$$\sum_{i=1}^{n} x_i = 1 \tag{4}$$

with the obvious constraints $0 \leqslant x_i \leqslant 1$. More conveniently, one can solve the polynomial:

$$c_1 x_1^n + c_2 x_1^{n-1} + \ldots + c_n x_1 - 1 = 0 \tag{5}$$

where the coefficients c_i are defined by the following recursive equation:

$$c_i = K_{A,n-i} c_{i+1}, \quad c_n = 1, \quad i = n-1, n-2, \ldots, 1 \tag{6}$$

For all positive values of K_i, there is only one real root meeting all the required constraints.

4.3. Model identification via spectroscopic modelling

Since the cluster composition of water is not experimentally available, a direct evaluation of equilibrium parameters of the proposed model is obviously not possible. The model can only be identified by simulating measurable phenomena which are affected by the presence of clusters in liquid water, and then comparing these results with experimental data. Raman spectra of liquid water, taken at various temperatures in the OH-stretching vibration region, have been used for this purpose before. Advanced spectrum deconvolution techniques have been applied to break up the observed spectrum into a series of spectral components, with each one believed to represent the contribution from a specific cluster (Bounaaj, 1990; Luu et al., 1982). Unfortunately, the deconvolution techniques, being only high-level curve-fitting methods, can be an art as much as a science. It has repeatedly been shown that the deconvolution of the Raman bands of liquid water is not unique, and that the spectra can be interpreted in various ways (Hornung, Choppin, & Renovitch, 1974). In this study, the spectral data will be processed and interpreted differently, based on the proposed model of clustering equilibrium in conjunction with a simple spectroscopic model.

According to Placzek's theory of Raman scattering, in the harmonic approximation the radiant intensity of a characteristic Raman line is proportional to N, the number of scattering molecules of the species in question in the sample (Long, 1977). For example, the scattering intensity for the jth vibrational mode ν_j, measured under parallel polarization (laser excitation and scattering geometry X(Z,Z)Y), is given by:

$$I_j^{||} \propto N \frac{(\nu_L - \nu_j)^4}{\nu_j\left[1 - \exp(-h\nu_j/kT)\right]}\left(45\bar{\alpha}_j'^2 + 4\bar{\gamma}_j'^2\right)L \tag{7}$$

where $\bar{\alpha}_j'^2$ and $\bar{\gamma}_j'^2$ are the invariants of the isotropic and anisotropic part of the symmetric polarizability tensor, respectively, and ν_L is the incident light frequency. The additional correction factor L results from the fact that the field strength $\in_s$ experienced by a fixed molecule is the sum of the incident field $\in_0$ plus a local field due to all the molecules except the fixed one. The Lorentz–Lorentz local field approximation predicts the following expression for this effect (Eckardt & Wagner, 1966):

$$L = (n_s/n_L)\left(n_s^2 + 2\right)^2\left(n_L^2 + 2\right)^2/81 \tag{8}$$

where n_s and n_L are the refractive indices of liquid water at the Stokes frequency $\nu_s = \nu - \nu_L$ and the incident frequency ν_L, respectively, both being functions of temperature and pressure (Harvey, Gallagher, & Levelt Sengers, 1998).

The isotropic part of the Raman spectrum, as opposed to its anisotropic part, gives information on vibrational relaxation processes in liquids that is not obscured by the simultaneous presence of rotational relaxation processes (Bratos & Tarjus, 1980). Therefore, the use of an isotropic part to interpret vibrational spectra is preferable. On the other hand, the experimental conditions only allow measurement of two spectral data sets that are proportional to either $45\bar{\alpha}_j'^2 + 4\bar{\gamma}_j'^2$ (X(Z,Z)Y) and $3\bar{\gamma}_j'^2$ (X(Z,X)Y) for the experiment utilizing an analyser or $45\bar{\alpha}_j'^2 + 7\bar{\gamma}_j'^2$ (X(Z,X+Z)Y) and $6\bar{\gamma}_j'^2$ (X(Y,X+Z)Y) when no analyser is used (Scherer, Kint, & Bailey, 1971). In each case, however, the isotropic spectrum can be obtained as a linear combination of the two independently measured experimental spectra.

Placzek's theory predicts no peak intensity spread around a given vibrational frequency ν_j. The measured spectral lines exhibit, however, a certain linewidth which is a summaric result of several simultaneous physical effects. The so-called natural linewidth, due to the Heisenberg uncertainty principle, is negligible. Doppler broadening arises from a Doppler shift caused by the motion of the molecule with respect to an incident photon. It is, by two-orders of magnitude, larger and accounts for about half of the spectral line broadening observed in dilute gas or vapour phase. Collision broadening or the Lorentz effect is caused by secondary interactions with other molecules or atoms. It was found to be a significant process at gas densities typical of the Earth's lower atmosphere and certainly becomes predominant in the much more condensed liquid phase. Other physical effects, such as resonance and Stark broadening seem to be less important. While Doppler broadening can be most simply characterised by a Gaussian function, the collision broadening used to be described by means of a Lorentzian function (Quine & Drummond, 2002; Scherer, 1978).

In the spectroscopic model which will be employed in this study to identify the chemical cluster model of liquid water, a product of a Lorentzian and Gaussian function is used to account for all possible linewidth broadening effects (Luu et al., 1982). Since for a species in solution, Eq. (7) implies proportionality to the molar concentration (Szymanski, 1967), the overall isotropic Raman intensity I_α, resulting from all vibrational modes ν_{ij} characterizing a mixture of n different water clusters will be:

$$I_\alpha(\nu) = \sum_{i=1}^{n}\sum_{j} x_i I_{\alpha,ij}(\nu)\phi_{ij}(\nu) \propto \frac{(\nu_L-\nu)^4 L}{\nu[1-\exp(-h\nu/kT)]}\sum_{i=1}^{n} x_i \sum_{j} S_{ij}\phi_{ij}(\nu) \quad (9)$$

where x_i is the mole fraction of ith cluster in the mixture and $S_{ij} = 45\bar{\alpha}_j'^2$ is the isotropic Raman scattering activity characterizing jth frequency mode of ith cluster. The Lorentzian–Gaussian distribution $\phi_{ij}(\nu)$ has been defined as follows:

$$\phi_{ij}(\nu) = \exp(-y)/(1+y) \text{ with } y = 1.224456\frac{\nu-\nu_{ij}}{w} \quad (10)$$

where w is the intensity peak width at half maximum. For the sake of simplicity, w was assumed to be the same for all frequency modes and cluster sizes (Krishnan et al., 1994). Although collision broadening is more likely to occur at higher fluid phase densities, the density dependence of w was neglected since the experimental spectra covered a relatively narrow density range (0.8–1 g/cm^3).

Eq. (9) involves three factors which are not specific to the mixture's molecular structure and composition. The Boltzmann population factor $[1-\exp(-h\nu/kT)]^{-1}$ accounts for the distribution of molecules having different vibrational quantum numbers (Szymanski, 1967). At temperatures of interest (above 250 K) in the OH-stretching vibration region, it is essentially unity and practically can be ignored. The term $(\nu_L-\nu)^4/\nu$ can be significant, since it leads to a 24% increase in intensity if the frequency changes from 3200 to 3600 cm^{-1}. Finally, the empirical refractive index correction for liquid water is about 2.5. It is worth noting that the three factors do not depend on the mixture composition (here, the cluster composition of water) and as such can be ignored in further analysis, provided their effect will also be eliminated from the experimental spectra (Scherer, 1978). Consequently, the theoretical Raman spectra were predicted in this study from the following equation:

$$\tilde{I}_\alpha(\nu) = \sum_{i=1}^{n} x_i \sum_{j} (S_\alpha)_{ij}\phi_{ij}(\nu) \quad (11)$$

The critical information required to use Eq. (11) effectively includes the vibrational frequencies ν_{ij}, the corresponding isotropic Raman activities $(S_\alpha)_{ij}$, the cluster composition of water x_i, and the half-width w of the Lorentzian–Gaussian distribution. The frequencies ν_{ij} and Raman activities $(S_\alpha)_{ij}$ were predicted by ab initio molecular simulation of small water clusters (from monomer to decamer). The cluster composition of water results from the proposed chemical equilibrium model of water clustering. The latter depends on the unknown constants of the van't Hoff equation, K°_{Ai} and ΔH_{Ai}. Together with the half-width w, they are adjustable parameters of the model. They will be determined by matching the predicted isotropic spectra of water with the corresponding experimental spectra at several different temperatures.

4.4. Molecular simulation of small water clusters

Despite the fact that spectral properties of small water clusters have been studied extensively over the past decade, the published data were found to be lacking. Information on vibrational frequencies, corresponding Raman activities, and thermochemical data for clusters ranging from water monomer to decamer, was insufficient. In order to create such a database, ab initio molecular simulations have been performed using the Gaussian 98 programme. Because of the limited available computing resources, a reasonable compromise had to be found between the accuracy of the selected model chemistry (the size of the basis set and the level of theory) and the required computational time. The optimised structure of water monomer was used as a selection criterion. The performed tests involved the (d) and (d,p) polarized basis sets 4-31G, 6-31G and 6-311G, with (+) and (+ +) diffuse functions. These were combined with the HF (Hartree–Fock self-consistent theory), MP2 (second-order Møller–Plesset perturbation theory), BLYP (Becke–Lee–Yang–Parr density functional theory) and B3LYP method. More than 80 different combinations have been tested. Some results of these comparative calculations are shown in Table 1. The list of predicted structural and spectral parameters of the water monomer included the total electronic energy E_0 (Hartree/molecule), the OH bond length r (Å), the HOH angle θ (deg) and the three key vibrational frequencies ν_i (cm^{-1}). They have been compared with the available experimental data to evaluate a mean error for each model chemistry. A combination of the 6-311+G(d,p) basis set and the BLYP DFT method was found to be the most effective model for the water monomer, giving a small average prediction error and acceptable computational time. It was decided, therefore, to use this molecular model for the simulation of small water clusters.

The structures of individual clusters were first optimized for the minimum total energy using Gaussian 98 with the tight SCF convergence option. Optimized cluster geometries from the Cambridge Cluster Database (Wales & Hodges, 1998), based on the empirical TIP4P potential, were used as an initial guess. The optimum clusters were found to have the same structures as predicted in earlier studies, i.e. a linear structure for the dimer, nearly planar cyclic structures for the trimer, tertramer and pentamer, a cage-like structure for the hexamer, and different three-dimensional structures for larger clusters.

The search for optimised cluster structures was followed by the harmonic vibrational analysis and thermochemistry calculations. Frequency and activity data calculated for the Raman spectral lines in the OH-stretching vibration region are shown in Table 2. It should be noted that Gaussian 98 predicts only the total Raman scattering activity (X(Z,X+Z)Y):

$$(S_{tot})_{ij} = 45\bar{\alpha}_{ij}^{\prime 2} + 7\bar{\gamma}_{ij}^{\prime 2} \tag{12}$$

and the depolarization ratio (Frisch, Yamaguchi, Gaw, & Schaefer, 1986):

$$\rho_{ij} = 3\bar{\gamma}_{ij}^{\prime 2} / \left(45\bar{\alpha}_{ij}^{\prime 2} + 4\bar{\gamma}_{ij}^{\prime 2}\right) \tag{13}$$

This information is sufficient, however, to determine the isotropic component of each spectral line from the following relationship:

$$(S_\alpha)_{ij} = \frac{3 - 4\rho_{ij}}{3\left(1 + \rho_{ij}\right)} (S_{tot})_{ij} \tag{14}$$

Fundamental frequencies computed with any model chemistry in the harmonic approximation are known to exhibit systematic errors. When anharmonicities are taken into account, overtone (higher harmonics) and

Table 1
Optimized structural parameters of water monomer—a comparison of various model chemistries

Model chemistry	E_0	r	θ	ν_1	ν_2	ν_3	% Error	CPU
4-31G(d,p)/BLYP	−76.3263776	0.9758	102.54	1643.77	3635.69	3747.45	1.32	10.43
6-31G/BLYP	−76.3666766	0.9892	106.63	1592.65	3446.14	3609.86	2.55	8.53
6-31G(d)/BLYP	−76.3885439	0.9799	102.72	1681.89	3569.10	3691.48	2.30	10.65
6-31G(d,p)/BLYP	−76.3988845	0.9763	102.69	1639.33	3644.36	3755.31	1.17	13.20
6-31+G(d,p)/BLYP	−76.4161391	0.9757	105.04	1569.70	3661.57	3782.50	0.82	14.88
6-311+G(d)/HF	−76.0377596	0.9404	108.14	1815.45	4127.35	4237.92	7.56	6.70
6-311+G(d)/MP2	−76.2447097	0.9594	107.59	1696.35	3827.24	3970.60	3.37	18.18
6-311+G(d)/BLYP	−76.4274869	0.9748	106.31	1627.14	3609.63	3727.44	1.28	17.62
6-311+G(d)/B3LYP	−76.4438091	0.9637	107.02	1667.43	3763.42	3881.04	2.32	9.80
6-311+G(d,p)/HF	−76.0533052	0.9412	106.22	1726.41	4141.85	4244.02	6.40	7.12
6-311+G(d,p)/MP2	−76.2747201	0.9595	103.47	1628.60	3883.62	4002.44	2.74	20.30
6-311+G(d,p)/BLYP	−76.4417019	0.9723	104.45	1571.41	3674.82	3780.21	0.72	18.45
6-311+G(d,p)/B3LYP	−76.4584627	0.9621	105.06	1602.85	3816.92	3922.19	1.73	11.20
6-311++G(d)/HF	−76.0379614	0.9404	108.15	1814.29	4127.22	4238.16	7.55	6.90
6-311++G(d)/MP2	−76.2449846	0.9593	107.61	1695.25	3826.49	3970.40	3.36	19.08
6-311++G(d)/BLYP	−76.4275913	0.9749	106.32	1626.00	3608.68	3726.98	1.28	18.58
6-311++G(d)/B3LYP	−76.4439291	0.9637	107.03	1666.34	3762.79	3880.83	2.31	10.53
6-311++G(d,p)/HF	−76.0534236	0.9412	106.22	1726.24	4142.56	4244.54	6.40	7.10
6-311++G(d,p)/MP2	−76.2749205	0.9595	103.46	1628.61	3884.54	4002.79	2.74	21.33
6-311++G(d,p)/BLYP	−76.4417634	0.9723	104.44	1571.24	3674.69	3779.98	0.72	19.32
6-311++G(d,p)/B3LYP	−76.4585308	0.9621	105.05	1602.66	3817.04	3922.18	1.73	12.42
Experimental[a]	−76.4802	0.9584	104.45	1594.59	3656.65	3755.79	–	–

Total electronic energy, E_0 (Hartree); O–H bond length, r (Å); H–O–H angle, θ (deg); vibrational frequencies, ν_i (cm^{-1}); average error (%); CPU time (arbitrary units).

[a] The experimental value of monomer energy as used by Kim et al. (1992); other data, including anharmonic frequencies, from Benedict, Gailar, and Plyler (1956)

Table 2
Raman spectral lines of small water clusters predicted from 6-311 + G(d,p)/BLYP model chemistry

Monomer: $E_0 = -76.4417018545$ Hartree			
3674.82	85.84	0.1360	61.86
3780.22	39.82	0.7500	0.00
Dimer: $E_0 = -152.892077434$ Hartree			
3554.98	190.98	0.1921	119.17
3675.03	78.33	0.1044	61.05
3749.68	54.76	0.4508	15.06
3775.50	33.81	0.7500	0.00
Trimer: $E_0 = -229.351014437$ Hartree			
3392.68	307.66	0.0881	249.53
3455.44	45.05	0.7354	0.51
3467.57	45.20	0.6405	4.02
3746.03	63.93	0.2842	30.92
3750.88	54.09	0.7235	1.11
3752.27	88.63	0.0952	70.65
Tetramer: $E_0 = -305.813644081$ Hartree			
3190.40	431.09	0.0914	346.85
3293.62	2.87	0.7500	0.00
3293.63	2.87	0.7500	0.00
3334.07	136.52	0.7500	0.00
3743.83	31.01	0.7500	0.00
3744.24	46.62	0.7500	0.00
3744.24	46.62	0.7500	0.00
3744.74	167.68	0.0071	164.92
Pentamer: $E_0 = -382.270727570$ Hartree			
3140.70	568.41	0.0881	461.03
3233.84	4.75	0.7497	0.00
3245.13	13.53	0.5059	2.92
3293.65	95.76	0.7453	0.34
3304.45	96.65	0.7330	1.26
3740.85	61.25	0.2918	28.97
3743.16	63.12	0.2541	33.28
3746.08	73.88	0.2124	43.68
3747.21	53.96	0.3290	22.79
3749.69	98.91	0.1439	69.88
Hexamer: $E_0 = -458.724325382$ Hartree			
3002.73	189.51	0.0965	150.59
3252.85	158.62	0.0941	126.79
3301.43	161.15	0.1263	118.99
3349.05	81.29	0.4977	18.26
3415.84	82.25	0.2858	39.59
3520.77	79.63	0.2614	41.13
3563.69	102.62	0.1817	65.81
3596.96	57.49	0.6039	6.98
3739.37	93.48	0.2566	48.94
3743.68	50.68	0.5075	10.87
3744.32	120.63	0.1028	94.39
3752.93	94.35	0.2483	50.56
Heptamer: $E_0 = -535.185199694$ Hartree			
2898.42	188.62	0.0988	149.05
3187.61	118.68	0.0992	93.69
3218.64	170.34	0.1089	131.30
3353.75	96.46	0.2950	45.19
3366.56	86.01	0.2448	46.54
3489.53	128.81	0.0461	115.56
3492.93	89.06	0.4416	25.40
3525.96	68.60	0.5252	13.48
3550.52	87.54	0.3623	33.22
3651.99	44.14	0.2286	24.98
3739.62	101.97	0.2165	59.62
3741.84	70.23	0.5253	13.79
3744.08	124.08	0.0907	100.00
3749.08	96.03	0.2341	53.52
Octamer: $E_0 = -611.651544933$ Hartree			
3005.78	434.56	0.0262	408.67
3033.47	72.52	0.7236	1.48
3064.87	2.02	0.7383	0.02
3067.74	2.05	0.7291	0.03
3455.72	60.98	0.7431	0.32
3459.49	1.95	0.7484	0.00
3460.40	2.54	0.5179	0.52
3472.01	394.71	0.0487	351.94
3482.79	185.14	0.6973	7.66
3512.14	8.27	0.7433	0.04
3513.45	8.10	0.7499	0.00
3529.75	60.59	0.7494	0.03
3737.75	66.23	0.5729	9.94
3737.88	55.94	0.6698	3.58
3737.96	118.63	0.1835	75.71
3738.20	196.66	0.0454	176.74
Nonamer: $E_0 = -688.109487169$ Hartree			
3005.71	579.37	0.0661	495.55
3027.08	38.32	0.2665	19.51
3035.19	5.70	0.5000	1.27
3099.42	10.33	0.7423	0.06
3143.08	54.15	0.7282	0.91
3444.30	20.02	0.7489	0.02
3449.03	9.16	0.2058	5.51
3467.49	424.44	0.0718	358.10
3470.38	55.84	0.7178	1.40
3471.87	114.04	0.6540	8.83
3475.65	131.84	0.7345	1.57
3524.31	1.25	0.4909	0.29
3526.07	15.60	0.6610	1.11
3737.69	82.53	0.2690	41.71
3738.42	46.84	0.4061	15.28
3738.60	158.90	0.1483	111.02
3740.37	120.46	0.1761	78.38
3749.31	94.23	0.1973	58.00
Decamer: $E_0 = -764.569506639$ Hartree			
2903.94	375.23	0.0531	331.09
2930.26	42.46	0.2789	20.86
3020.82	138.95	0.0730	116.89
3024.04	36.72	0.5061	7.93
3253.20	17.73	0.2482	9.50
3286.36	197.00	0.1984	120.90
3422.56	61.16	0.7179	1.52
3426.31	76.30	0.1545	52.47
3452.78	121.39	0.6740	7.35
3453.85	182.88	0.0137	177.11
3487.38	116.61	0.1683	77.42
3492.93	81.36	0.6935	3.62
3513.40	29.70	0.5978	3.77
3557.74	44.90	0.2039	27.16
3570.93	116.09	0.3256	49.56
3735.80	65.52	0.3299	27.60
3736.34	102.80	0.2378	56.72
3737.67	77.91	0.3807	27.79
3737.91	137.53	0.0905	110.90
3740.03	121.77	0.1512	84.45

Data given in the following order: unscaled harmonic frequency, cm^{-1}; total scattering activity, $Å^4$/amu; depolarization ratio, (–); isotropic scattering activity, $Å^4$/amu.

Table 3
Ideal gas phase enthalpies of small water clusters and clustering reactions

Cluster	H_i (Hartree)	ΔH_{Ai} (kJ/mol)	ΔH_{Ai} (kJ/mol)
	This work		Quintana et al. (1998)
Monomer	−76.4174	–	–
Dimer	−152.8406	−15.50	−24.27
Trimer	−229.2720	−36.86	−48.18
Tetramer	−305.7074	−47.22	−40.17
Pentamer	−382.1374	−33.32	−30.73
Hexamer	−458.5633	−22.36	−25.49
Heptamer	−534.9966	−41.86	−39.40
Octamer	−611.4350	−55.22	−42.86
Nonamer	−687.8661	−36.26	−42.60
Decamer	−764.2987	−39.77	n.a.

combination frequencies are also permitted. Fortunately, in Raman spectra, unlike infrared spectra, such bands are typically much weaker than the fundamentals (Long, 1977). It is common practice to apply certain scaling factors to bring the calculated frequencies closer to their experimental values. The optimal scaling factors vary by the basis set and theory level employed. Foresman and Frisch (1996) report some recommended values for a number of models. Unfortunately, a reliable value for the 6-311+G(d,p)/BLYP model could not be found. The scaling factor $\zeta = \nu_{exp}/\nu_{calc}$ can be determined from the results of vibrational analysis for the water monomer and relevant experimental data. The experimental anharmonic OH-stretching frequencies from Table 1 and the theoretical frequencies 1571.42, 3674.82 and 3780.22 cm^{-1}, give ζ factors of 1.0147, 0.99506 and 0.99354, respectively. Since the resulting values differ from each other and, in addition, since there is some controversy on whether anharmonic or harmonic experimental frequencies should be used in this comparison, it was decided that ζ should be considered an adjustable parameter of the spectroscopic part of the proposed model.

Thermochemical calculations have also been performed in order to estimate the incremental enthalpies of water clustering ΔH_{Ai}. Gaussian 98 enables one to calculate the sum of electronic and thermal enthalpy per cluster molecule, H_i (Hartree/molecule), at 298 K. The enthalpy of the clustering reaction given by Eq. (1) can then be determined as follows:

$$\Delta H_{Ai}[\text{kJ/mol}] = 4.184 \times 627.5095 \times (H_{i+1} - H_i - H_1),$$
$$i = 1, 2, \ldots, 9 \qquad (15)$$

One has to bear in mind, however, that results of the above thermochemical analysis are valid for non-interacting molecules and, in principle, apply to an ideal gas situation only. The calculated values of H_i and ΔH_{Ai} are shown in Table 3. The ab initio clustering enthalpies have been compared with results obtained by Quintana, Ortiz, and López (1998) who used the empirical interparticle TIP4P potential. The latter had to be extrapolated from very low temperatures to 298 K. Although some discrepancies are evident, the general trends observed with the growing cluster size are similar in both approaches. Since empirical methods are known to show large divergences in vibrational properties, depending on the empirical potential used (especially in problems involving hydrogen bonding), the ab initio results obtained in this work were found to be preferable. Due to the ideal gas assumption, however, all enthalpies given by Eq. (15) will still be refined as part of the parameter estimation procedure.

4.5. Experimental Raman spectra of liquid water

A vast amount of experimental spectral data for liquid water in the stretching vibration region has accumulated over the years. Table 4 gives a comprehensive list of the published Raman spectra, taken at different temperatures and pressures. It is understandable, that the precision of early studies, especially those from the pre-laser era involving mercury-excited photoelectric spectra, cannot comply with modern measurement standards. Therefore, they have to be considered less reliable. In addition, a series of studies were performed only at one ambient temperature, often without paying too much attention to strict temperature control. In certain cases, only one type of Raman spectrum was recorded (or published), making the evaluation of the isotropic component impossible. In a few others, the information provided was simply insufficient to identify the spectrum type. In addition, some authors who measured spectra at various temperatures and were only interested in the correct band assignment, normalized spectral curves in such a way that the effect of temperature on scattering intensity could not be evaluated. A thorough analysis of the individual data sets led to the selection of spectra from the following five studies: Scherer, Go, and Kint (1974), D'Arrigo, Maisano, Mallamace, Migliardo, and Wanderlingh (1981), Ratcliffe and Irish (1982), Walrafen, Hokmabadi et al. (1986), and Hare and Sorensen (1990). A database of 34 spectral curves was created covering a wide range of temperatures, from −30 to 250 °C. Although the most reliable data have been selected for the model validation, the possibility of experimental errors could not be entirely eliminated. Fig. 1 shows, for example, some systematic differences existing between spectra reported by Scherer et al. (1974) and two other authors at −10 °C.

The selected spectra have been scanned from the original publications and then converted to numerical data. Before being used in the cluster model identification, the data were corrected for the Boltzmann population factor, $(\nu_L - \nu)^4/\nu$ frequency factor, refractive

Table 4
Experimental studies reporting Raman spectra of liquid water

Authors	Year	Temperature [C]/pressure [bar][a]	Type of published spectra	Light source	Incident light		Corrections made[b]	Notes[b]
					Wavelength [nm]	Power [W]		
Rao	1931	14, 75		Hg				
Rao	1934	0, 4, 38, 98		Hg				
Cross, Burnham, and Leighton	1937	26, 75, 40, 310/?, 374/220	X(ZZ)Y	Hg–Ar	253.7			
Busing and Hornig	1961	25	?	Hg	435.8			
Schultz and Hornig	1961	2, 25, 95	?	Hg	435.8			
Weston	1962	~(25–35)	depolar. ratio	Hg	435.8			
Walrafen	1964	8, 28, 80; 25	X(Y+Z, X+Z)Y ?	Hg	435.8			
Kęcki, Witanowski, Akst-Lipszyc, and Minc	1966	2, 25, 90	?	Hg	404.7			
Rao and Ramanaiah	1966	25, 55, 90	X(ZZ)Y, X(ZX)Y	Hg	491.6			
Walrafen	1967	10, 30, 50, 70.2, 90	X(Y+Z, X+Z)Y	Hg	435.8			
Colles, Walrafen, and Wecht	1970	5, 85	X(ZZ)Y ?	Nd^{3+}	530.0			
Lindner	1970	400						
Walrafen	1970	25	X(ZZ)Y ?	Ar^{+}	488.0	1		
		25	X(Y+Z, X+Z)Y ?	Hg	435.8	?		
Murphy and Bernstein	1972	25	X(ZZ)Y iso-, anisotropic	Ar^{+}	488.0	0.70		
Cunningham and Lyons	1973	2.1, 21.1, 41, 59.1, 87.7	X(ZZ)Y, X(ZX)Y	He–Ne	632.8 ?	0.075	B, I	
Scherer, Go, and Kint	1973	23, 90	iso-, anisotropic	Ar^{+}	514.5	0.04–0.5	F, T	*T*-norm.
Scherer, Go, and Kint	1974	−10, 10, 30, 50, 70, 90, 23	iso-, anisotropic	Ar^{+}	488.0	?	F, T	
Walrafen	1974	25	X(ZZ)Y, X(ZX)Y, isotropic	Ar^{+}	476.5	0.28		scale
Sceats, Rice, and Butler	1975	23, 62	X(ZZ)Y, X(ZX)Y	Nd^{3+}	530.8			
Kint and Scherer	1978	–10.3	Iso-, anisotropic	Ar^{+}	514.5	0.25		
Moskovits and Michaelian	1978	~20 ?	X(ZZ)Y, X(ZX)Y	Ar^{+}	488.0	0.7		
Luu, Luu, and Boiron	1980	−15, 25, 45, 85, 120	X(ZZ)Y	Ar^{+}	514.5	0.10		
D'Arrigo et al.	1981	−24, −16, −10, 0, 10, 20, 40, 60, 80, 95	isotropic	Ar^{+}	514.5	0.3	B, F, T, D, R	
Bekkiev and Fadeev	1982	10, 20, 33, 55	?	Nd^{3+}	532	?	?	*T*-norm.
		20, 40, 65	depolar. Ratio					
Ratcliffe and Irish	1982	4, 21, 50, 100/s, 150/s, 200/s, 250/s, 300/s	X(Z,X+Z)Y iso-, anisotropic	Ar^{+}	488.0		D	
Yeh, Bilgram, and Känzig	1982	−21, 5.3 (iso-), −11.2 (aniso-)	iso-, anisotropic	Ar^{+}	514.5	0.15	F, T	
Giguere and Chen	1984	4, 45	polarizer/scrambler	Ar^{+}	488.0	?		
Giguere and Pigeon-Gosselin	1986	~20	X(ZZ)Y					
Green, Lacey, and Sceats	1986	−25, −10, 10, 30, 50, 70, 90	X(ZZ)Y, X(ZX)Y	Ar^{+}	514.5	0.2		scale area-norm.
Walrafen, Fisher et al.; Walrafen, Hokmabadi et al.	1986	3, 22, 42, 58, 72	X(ZZ)Y	Ar^{+}	?			
		4, 22, 42, 59, 72	X(ZX)Y					
		3, 21, 44, 60, 72	X(Z,X+Z)Y					
		3, 22, 42, 60, 72	X(Y,X+Z)Y					
		5, 24, 48, 68, 85	X(Y+Z,X+Z)Y					
Zhelyaskov, Georgiev, and Nikolov	1988	4, 20, 40, 60, 80, 90	iso-, anisotropic	Ar^{+}	514.5	?	F, T	scale *T*-norm.
Brooker, Hancock, Rice, and Shapter	1989	25	X(ZZ)Y, X(ZX)Y	Ar^{+}	?	0.4−0.6	F, T	
Seuvre	1989	~20						
Sokołowska	1989	2, 45	iso-, anisotropic	Ar^{+}	488.0	0.1	F, T	scale *T*-norm.
Bounaaj	1990	−13,−8,−3, 27, 47, 67, 87, 107/s, 127/s	X(ZZ)Y ?					

(*continued on next page*)

Table 4 (*continued*)

Authors	Year	Temperature [C]/pressure [bar][a]	Type of published spectra	Light source	Incident light Wavelength [nm]	Incident light Power [W]	Corrections made[b]	Notes[b]
Hare and Sorensen	1990	−30, −20, −10, 0, 20, 40, 60, 80	X(ZZ)Y, X(ZX)Y	Ar^+	488.0	0.07		isosb-norm
Luu, Cambon, and Mathlouthi	1990	20	X(ZZ)Y, X(ZX)Y	Ar^+	488.0	0.15		
Kohl, Linder, and Franck	1991	25, 100, 200, 300, 400/ (density, g/cm^3) 1.0, 1.0, 1.0, 0.9, 0.8	isotropic	Kr^+	647.1	6	F, T ?	
Frantz, Dubessy, and Mysen	1993	1, 4, 10, 21, 40, 60, 80; from 100/227 to 505/2023	X(Z,X+Z)Y?	Ar^+	514.5	1.8	T	*T*-norm.
Serghat	1993	~20						
Chatzidimitriou-Dreismann, Krieger, Moeller, and Stern	1995	~20	X(Z,X+Z)Y	Ar^+	514.5			
Carey and Korenowski	1998	24/128, 200/256, 400/256	X(ZZ)Y	Ar^+	514.5	0.5	T, B	
Hutteau	1998	~20	X(ZZ)Y					
Durig et al.	1999	7, 60, 88	X(ZZ)Y, X(ZX)Y	Ar^+	514.5			

[a] Pressure shown only if different from atmospheric; /s, saturated vapour pressure.

[b] B, baseline subtraction, F, frequency correction, T, correction for the Boltzmann population factor, D, density correction, R, refractive index correction; *T*-norm, peak normalization for all isotherms; isosb-norm, normalized to cross at 3403 cm^{-1}, the Walrafen isosbestic; scale, intensity scale not available.

index, and density (unless some of these corrections had already been made by the authors). For density correction, the observed spectrum is divided by the relative density of liquid water at a particular temperature and pressure. This gives approximately the intensity scattered from a fixed number of water molecules per unit volume (Ratcliff & Irish, 1982).

4.6. Parameter estimation

The results of vibrational analysis of small water clusters, when compared with experimental Raman spectra of liquid water, can provide some general guidance on the significance of individual species in a mixture at different temperatures. Fig. 2 presents theoretical spectral lines of investigated clusters, together with two experimental spectra of liquid water placed in the background (line intensities have been divided by the corresponding cluster size to properly reflect their significance). A closer inspection of Fig. 2 clearly shows that it is impossible to incorporate proposed model clusters larger than hexamer. This is due to their high activity below 3100 cm^{-1} where even supercooled water reveals merely some residual Raman scattering (possibly attributed to a medium-intensity line of hexamer at 3002 cm^{-1}). Despite this failure, the key features of the observed spectra can be successfully interpreted by means of spectral lines of clusters smaller than heptamer. For example, the peak intensity of the spectrum at −30 $^\circ$C corresponds to a high-intensity line of tetramer at 3190 cm^{-1}, although a certain contribution from the neighbouring pentamer line (3141 cm^{-1}) cannot be excluded (see Fig. 2). Similarly, the peak intensity at 250 $^\circ$C can be attributed to a high-intensity line of dimer at 3555 cm^{-1}. Some features of the fine structure of liquid water spectra can also be explained. The well-known shoulder observed at low temperatures around 3400 cm^{-1} seems to be caused by a strong 3393 cm^{-1} line belonging to trimer, whilst a weaker shoulder at about 3260 cm^{-1} found at high temperatures, is probably due to two lines of hexamer present in this region (3253 and 3301 cm^{-1}). Based on the earlier qualitative arguments, the original model involving molecules from monomer to decamer has been reduced, so as not to contain clusters larger than hexamer.

The model parameters were estimated by non-linear regression using a standard least-squares performance index. Experimental spectra were composed of approximately 600–1700 points each. Both the experimental and predicted spectra belonging to a given data set (study) were normalised to allow data comparison. The peak intensity taken from the lowest temperature spectrum within each data set (involving several isotherms) was used as a reference value for all isotherms. The simplex optimization method was employed to minimize the performance index.

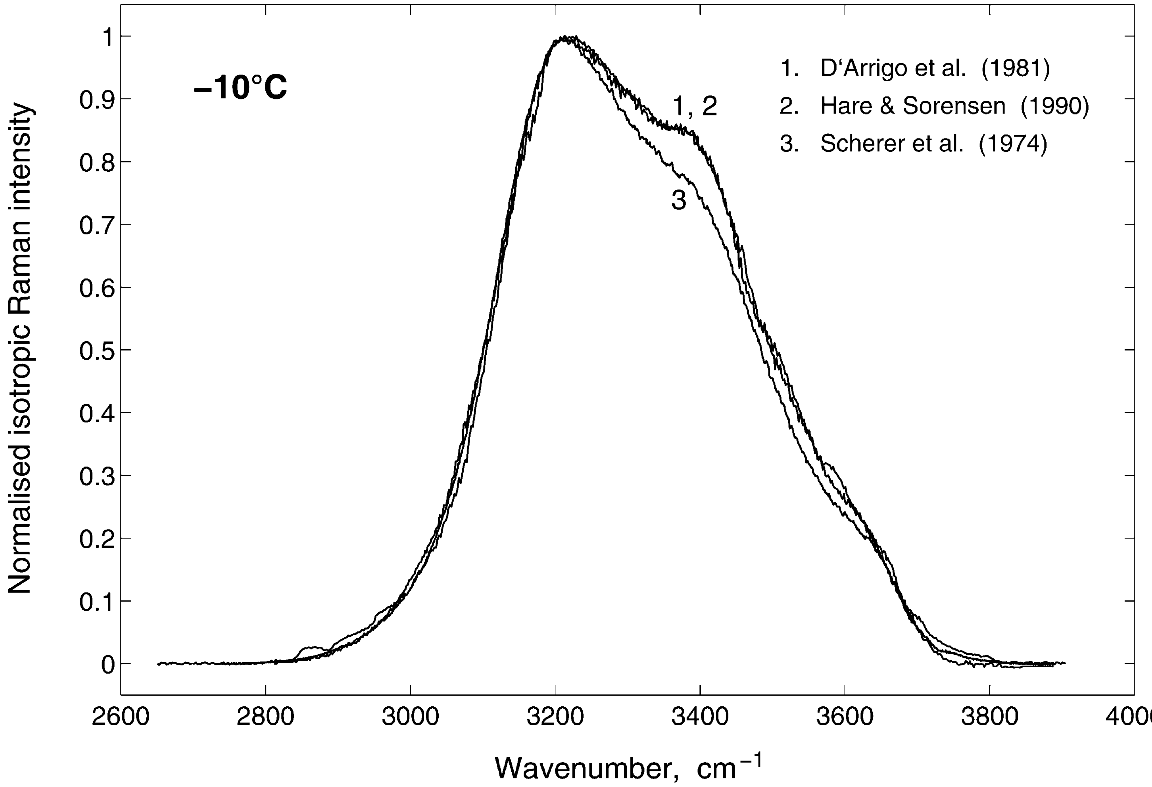

Fig. 1. Raman spectra of liquid water from different experimental studies at −10 °C.

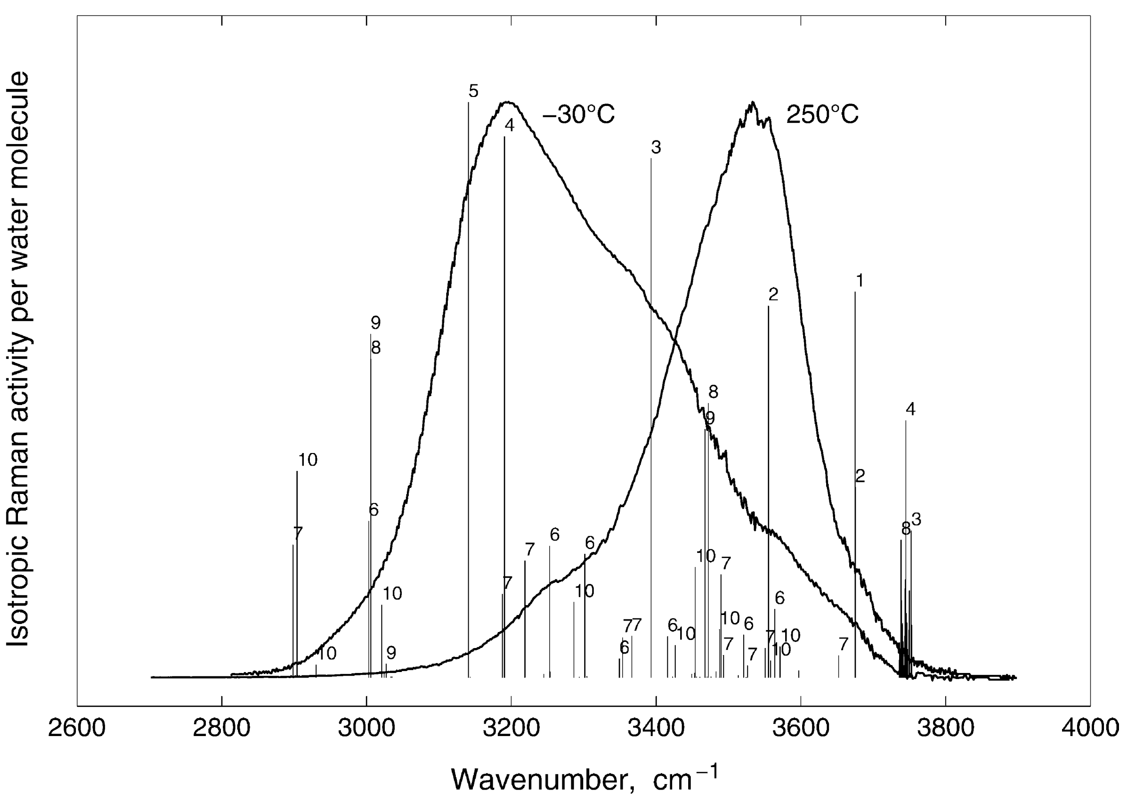

Fig. 2. Spectral lines of small water clusters obtained from 6-311+G(d,p)/BLYP model chemistry. Numbers next to the lines indicate the size of the cluster exhibiting the given frequency mode. To facilitate comparison, the calculated activities have been divided by the cluster size. Experimental spectra at extreme temperatures, −30 and 250 °C, are also shown.

Preliminary calculations showed that matching the experimental spectra with the proposed model over the entire stretching vibration region, over a very broad range of temperatures, was not possible. The problem arises in a relatively narrow frequency region (3740–80 cm^{-1}) representing the asymmetric stretching vibration band. According to theoretical calculations, isolated water clusters from trimer to decamer exhibit a series of fairly active lines at these frequencies (see Table 2). This is contrary to the continuous experimental spectra of bulk water which, irrespective of temperature, show no Raman activity in this region. Such a conflicting situation becomes critical at low temperatures when the concentration of larger clusters is expected to be high. With increasing temperature the problem disappears, since by then the concentration of larger clusters decreases, whilst isotropic spectral lines of monomer and dimer in this region are Raman-inactive. Because the above controversy was not resolved, it was eventually decided that only spectral lines of small clusters in the major part of the stretching vibration region (2700–3700 cm^{-1}) should be considered, and those representing asymmetric stretching vibrations (above 3700 cm^{-1}) should be ignored.

The results of data fitting are shown in Fig. 3. The predicted values of isotropic Raman intensity have been plotted against their experimental values at several temperatures, forming a series of correlation curves. In general, the data fit is satisfactory. Larger deviations are observed only at extreme conditions, that is at temperatures above 150 °C and, to a smaller extent, below −20 °C. According to the experimental data by Ratcliffe and Irish (1982), selected for this study, the high-temperature water exhibits a sharp increase of Raman intensity with increasing temperature. Although the model also predicts a certain increase in this region, it still appears to be insufficient to match the data at the peak intensity. It has to be noted, however, that high temperature experimental spectra reported by Lindner (1970) and more recently by Carey and Korenowski (1998) show an opposite trend, that is a decrease of the peak intensity with temperature. In turn, peak intensities predicted by the model for the supercooled water are very close to their experimental values. Unfortunately, they are slightly right-shifted (by about 50 cm^{-1}), resulting in systematic errors in the least-squares sense (Figs. 4 and 5). A very good data fit was obtained for the broad intermediate temperature range (0–100 °C), where even the fine structure of spectral curves has been properly reproduced, including a right shoulder feature for 0–25 °C and left shoulder feature for 30–100 °C (see Fig. 4). The existence of the isosbestic point was also confirmed (Fig. 6). A rather poor fit was obtained for the right tail of the spectra, where the intensity predicted by the model at all temperatures is evidently higher than the observed residual intensity. To some extent, however, the observed inconsistencies can be attributed to the inaccuracy of experimental data.

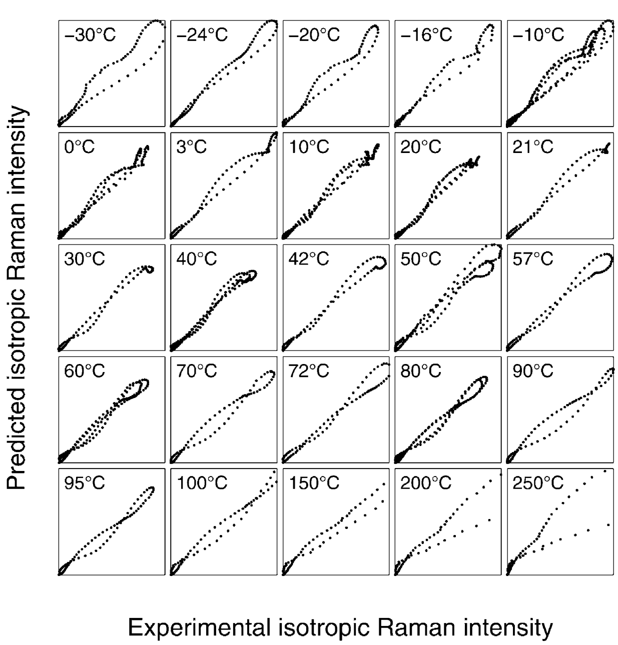

Fig. 3. Correlation diagrams of spectral curves at different temperatures.

The numerical values of estimated parameters of the model are shown in Table 5. As expected, the enthalpies of water clustering were found to be substantially different from those predicted by molecular simulation for the ideal gas phase. They all remained negative, however, indicating the exothermic nature of clustering reactions. In fact, all the enthalpies given in Table 5 compare very well with the typical energy values of 15–25 kJ/mol-H bond reported for O–HO bonds in the liquid phase (Pimentel & McClellan, 1960). The two auxiliary parameters associated with the spectroscopic model, the scaling factor ζ and half-width w, were 1.0211 and 229.2 cm^{-1}, respectively.

5. Cluster composition of liquid water

Knowledge of equilibrium constants at any temperature allows for the prediction of the cluster composition of liquid water as a function of temperature. Mole

Table 5
Estimated parameters of the van't Hoff equation for water clustering reactions

I	Reaction step	Equilibrium constant at 25 °C, K°_{Ai}	Enthalpy of reaction, ΔH_{Ai} [kJ/mol]
1	$H_2O + H_2O = (H_2O)_2$	1508.5	−25.574
2	$(H_2O)_2 + H_2O = (H_2O)_3$	2292.5	−19.010
3	$(H_2O)_3 + H_2O = (H_2O)_4$	90.662	−23.798
4	$(H_2O)_4 + H_2O = (H_2O)_5$	91.179	−19.177
5	$(H_2O)_5 + H_2O = (H_2O)_6$	24.588	−31.217

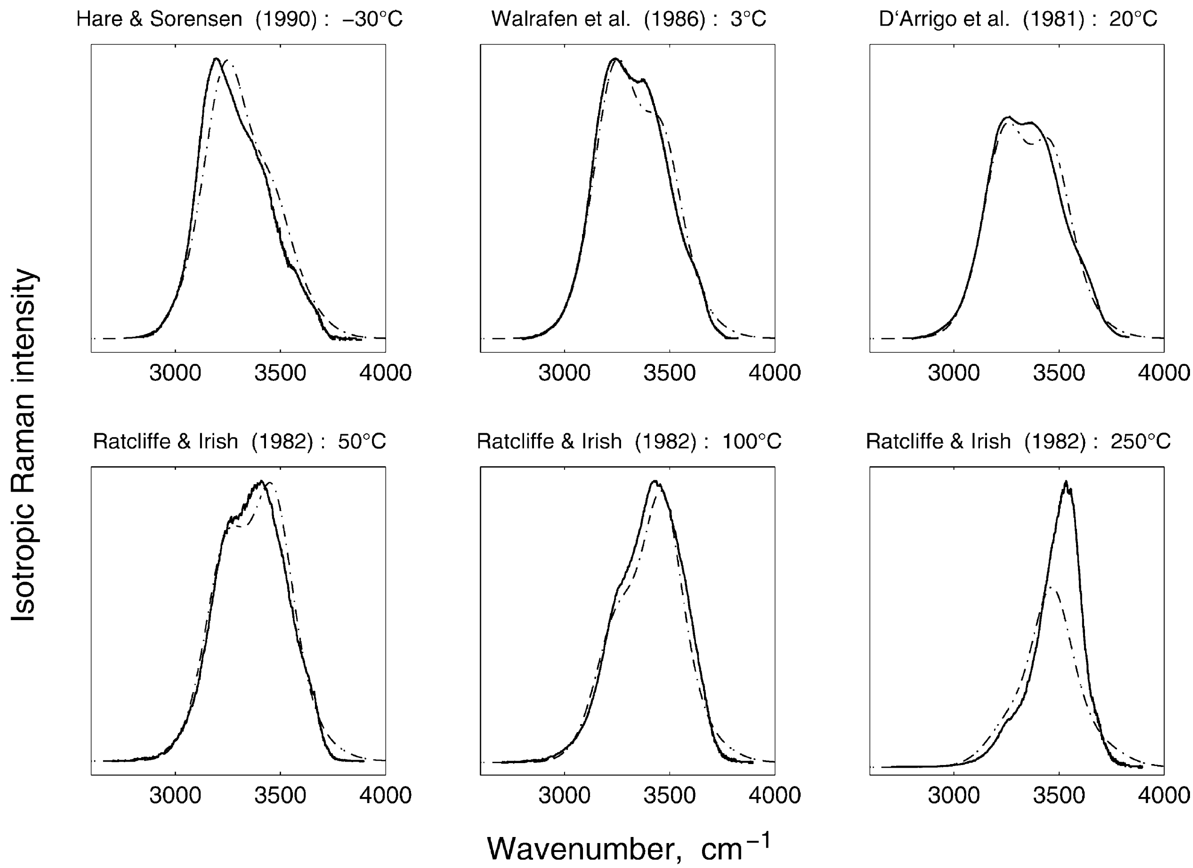

Fig. 4. Selected results of spectral curve fitting (solid lines, experimental spectra; broken lines, predicted spectra).

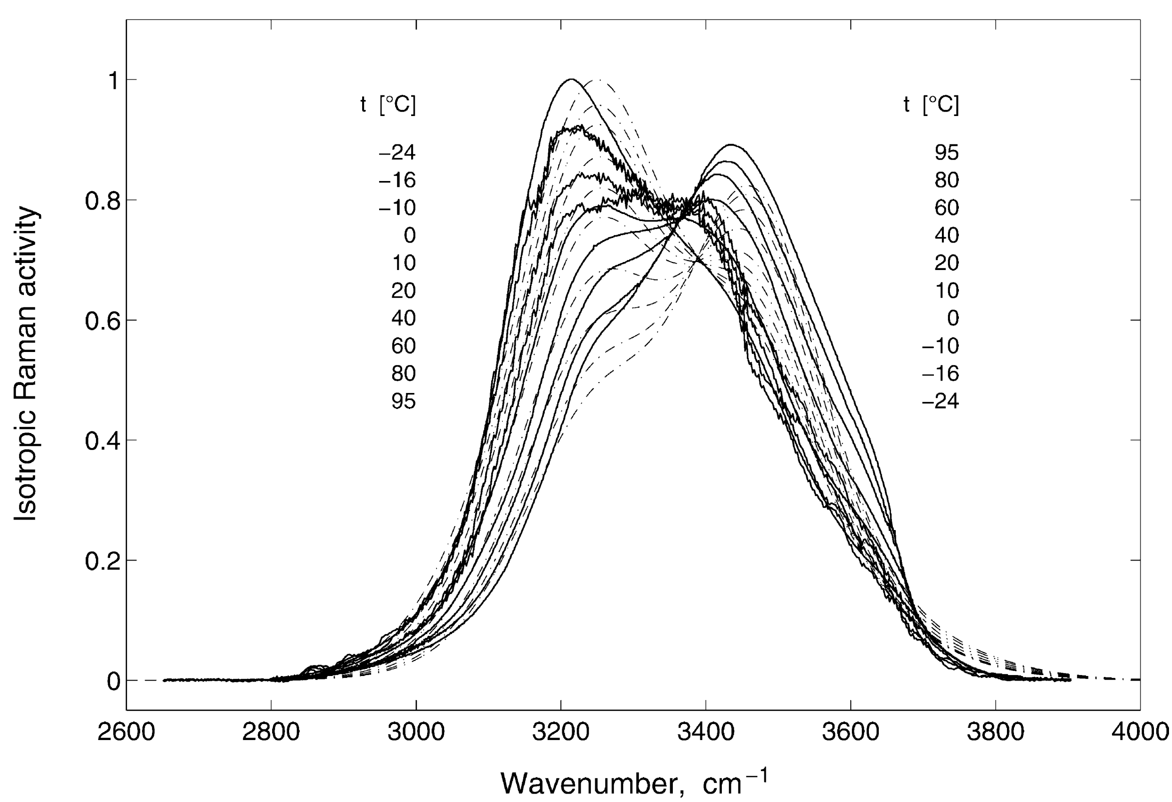

Fig. 5. Comparison of model predictions (broken lines) with the experimental data of D'Arrigo et al., 1981 (solid lines).

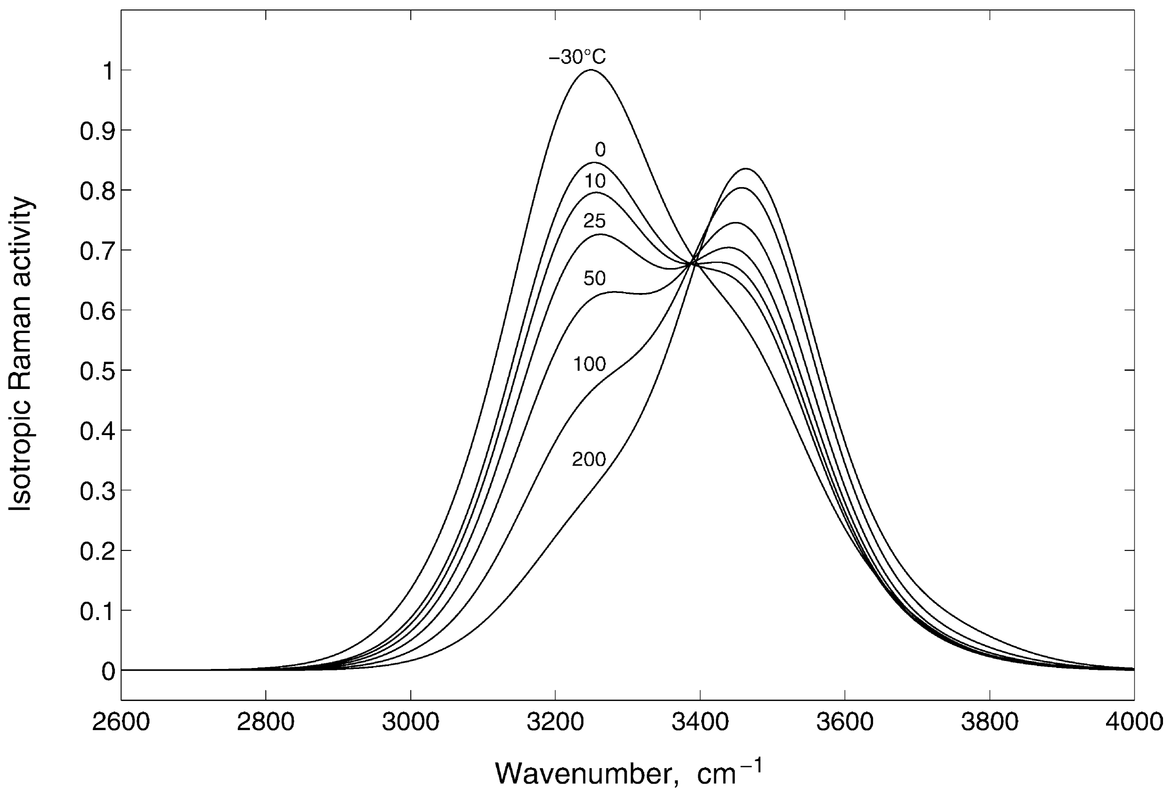

Fig. 6. Raman spectra of liquid water predicted at several temperatures.

fractions of individual clusters can be calculated from Eqs. (3) and (5). The cluster composition of water can be alternatively expressed in terms of the so-called analytical mole fractions $(x_i)_{\mathrm{anal}}$, which are based on the number of H_2O molecules involved rather than the number of clusters. The following conversion then obviously applies:

$$(x_i)_{\mathrm{anal}} = \frac{ix_i}{\sum_{j=1}^{n} jx_j} \tag{16}$$

where x_i is the cluster-based mole fraction.

The simulation results of the cluster composition of water for temperatures ranging from −50 to 350 °C are shown in Fig. 7. The qualitative picture of the cluster composition of liquid water, obtained from the proposed model, agrees well with some experimental data obtained using various techniques. Calculation results show a very low concentration of water monomer (below 1 mol%) at temperatures below 100 °C. This is in line with early observations by Stevenson (1965) based on three independent pieces of evidence, such as the vacuum ultraviolet absorption spectra of water vapour and liquid, the semi-empirically calculated heat and entropy of solution of water monomer in liquid water, and the lack of structure at 1.89–1.90 μ of the broad 1.90 μ band of the near-infrared absorption spectrum of liquid water. A relatively small concentration of non-bonded water resulted also from the study by Bonner and Woolsey (1968) who investigated spectra of liquid water at 25 °C over the range 0.6–1.8 μ. Model predictions are also consistent with the infrared spectroscopic measurements indicating that the monomer concentration systematically increases with increasing temperature. A similar trend is predicted for water dimer. According to the model, trimer is the predominant cluster over a wide range of temperatures, probably from the melting point up to the critical point, with a flat maximum at about 205 °C. The predicted high concentration of water trimer (above 50 mol%) confirms the results of measuring the tracer diffusion coefficient of ^{18}O-substituted water (Easteal, Vernon, Edge, & Wolf, 1984) according to which the average size of mobile clusters in liquid water at ambient temperatures is around 3. The correlated motion of three water molecules was also reported by Hawlicka and Grabowski (1992). On the other hand, the well-known and very accurate X-ray diffraction experiments of Narten, Danford, and Levy (1967) demonstrated a considerable degree of short-range order in liquid water, characterized by a coordination number (number of the immediate neighbours) of about 4.4 at temperatures from 4 to 200 °C. The persistence of the tetrahedral arrangement would indicate the presence of structures larger than trimers, such as tetramers, pentamers and hexamers. For example, the recent experiments by the Saykally group (Liu, Cruzan et al., 1996) involving the VRT (vibration–rotation–tunnelling) spectroscopy technique revealed

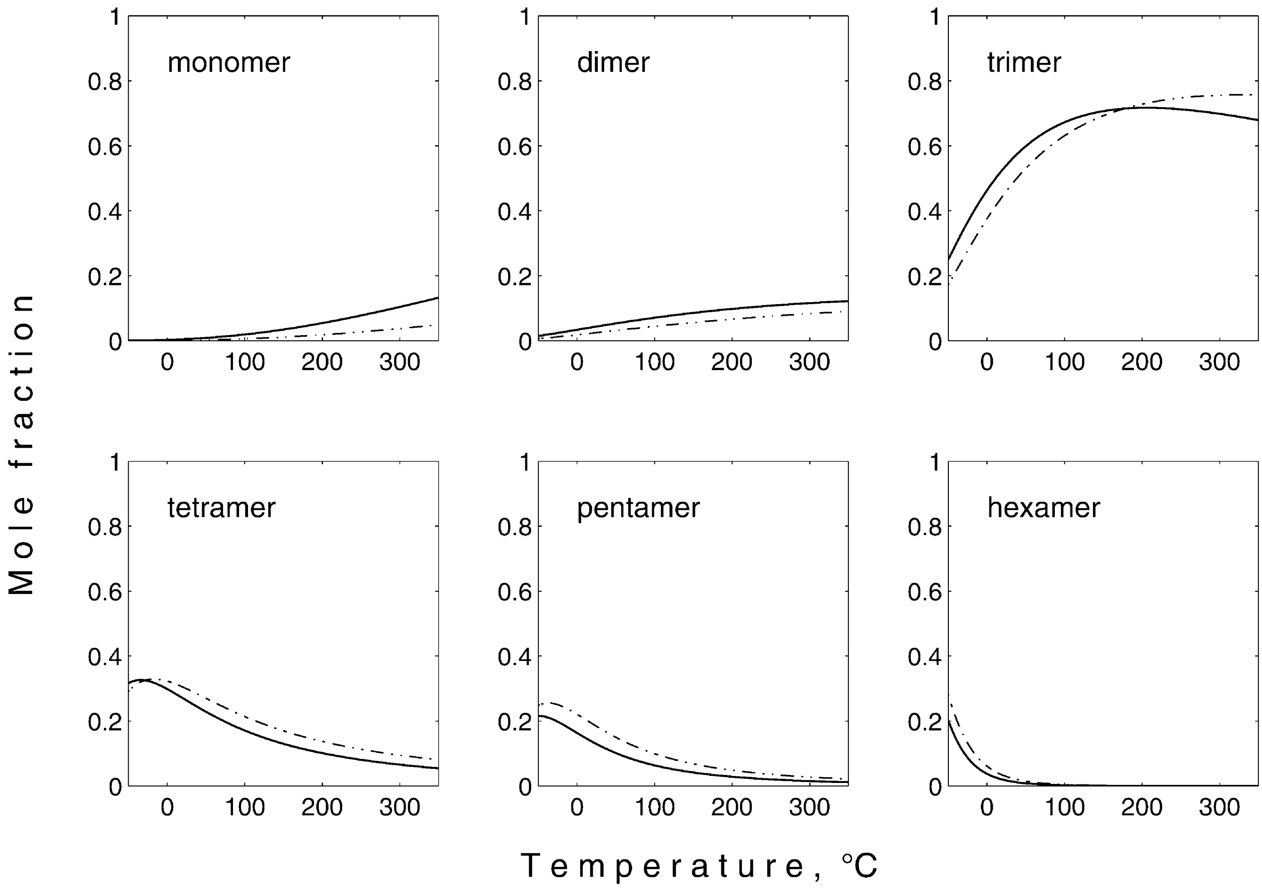

Fig. 7. Cluster composition of liquid water as a function of temperature (solid lines, cluster-based mole fraction; broken lines, analytical mole fraction).

that the average distance between the oxygen atoms in the cage hexamer (2.85 Å) is very close to that in bulk water, and the charge distribution is also very similar. These facts suggest that the cage-like hexamer plays a key role in determining the overall properties of water, including its amazing ability to dissolve other chemical compounds. The cage hexamer, due to its three-dimensional geometry and a highly uneven distribution of electrostatic charge, can encapsulate the solute molecule and tear it apart into constituent ions. The calculated tetramer concentration assumes a maximum of 33 mol% (analytic) at about −17 °C. Pentamer shows a similar pattern with a maximum of about 25 mol%. Hexamer, the largest accepted cluster of the model, is the most abundant cluster in highly supercooled liquid. Its predicted concentration becomes negligible above 50 °C.

6. Conclusion

The proposed model of water clustering in the condensed phase is based on the key assumption that the liquid water is a thermodynamically ideal mixture of small water clusters in a state of chemical equilibrium. The model has been validated using experimental Raman spectra, of liquid water in the stretching vibration region at different temperatures. The corresponding theoretical spectra were obtained by superposition of individual cluster spectra, assuming their composition-based additivity. For the spectroscopic modelling, Placzek's model of Raman scattering, extended to multicomponent mixtures, was used. Raman spectral lines of isolated water clusters were obtained from ab initio molecular simulations employing the 6-311+G(d,p) basis set and BLYP method. In order to obtain continuous spectra, the broadening of individual spectral lines was described by the Lorentzian–Gaussian distribution around the peak value. Although, initially, water clusters up to decamer were considered as possible candidates, having hexamer as the largest cluster was found sufficient to fit the spectral data satisfactorily. This does not mean, of course, that considering clusters larger than decamer would not lead to a more predictable model. The most recent speculative conceptual models of liquid water structure by Chaplin (1999) and Johnson (2000) suggest the existence of large dodecahedral "buckyball-like" clusters composed of twenty and more water molecules. Unfortunately, to the best of our knowledge, their Raman spectral lines have not yet been published.

The cluster composition of liquid water predicted by the model is also qualitatively consistent with several independent pieces of experimental data (NIR absorption spectra, self-diffusion coefficient, X-ray diffraction, VRT spectroscopy). Bearing in mind, however, that a number of simplifying assumptions had to be made to develop the model, the quantitative results can easily be questioned. Therefore, to be accepted, the model still requires an independent verification, involving, for example, the prediction of selected physical properties of liquid water. At the current stage of development, the authors perceive the proposed model as a new, certainly more rational and rigorous version of the conventional spectrum deconvolution technique rather than a definite model of water structure.

Acknowledgements

Partial financial support of this study from the Association Andrew van Hook for the Advancement of the Knowledge on Sugar, Reims (France), is greatly acknowledged.

References

Angell, C. A. (1971). Two-state thermodynamics and transport properties for water as zeroth-order results of a "bond lattice" model. *J. Phys. Chem.*, *75*(24), 3698–3705.

Arakawa, K., Tokiwano, K., & Kojima, K. (1977). Statistical thermodynamic theory of liquid water. *Bulletin of the Chemical Society of Japan*, *50*(1), 65–75.

Bekkiev, A. J., & Fadeev, V. (1982). V Effect of temperature, salts, and acids on the shape of Raman lines of water. *Doklady Akademii Nauk SSSR*, *262*(2), 328–331.

Belch, A. C., & Rice, S. A. (1987). The distribution of rings of hydrogen-bonded molecules in a model of liquid water. *J. Chem. Phys.*, *86*(10), 5676–5682.

Benedict, W. S., Gailar, N., & Plyler, E. K. (1956). Rotation-vibration spectra of deuterated water vapor. *J. Chem. Phys.*, *24*(6), 1139–1165.

Ben-Naim, A., & Stillinger, F. H. (1972). Aspects of the statistical-mechanical theory of water. In R. A. Horne (Ed.), *Water and aqueous solutions. Structure, thermodynamics, and transport processes* (pp. 295–330). New York: Wiley-Interscience.

Benson, S. W., & Siebert, E. D. (1992). A simple two-structure model for liquid water. *J. Am. Chem. Soc.*, *114*(11), 4269–4276.

Bernal, J. D. (1964). The structure of liquids. *Proc. Roy. Soc. (London)*, *A280*(1382), 299–322.

Bernal, J. D., & Fowler, R. H. (1933). A theory of water and ionic solution, with particular reference to hydrogen and hydroxyl ions. *J. Chem. Phys.*, *1*(8), 515–548.

Bjerrum, N. (1952). Structure and properties of ice. *Science*, *115*(2989), 385–390.

Bonner, O. D., & Woolsey, G. B. (1968). The effect of solutes and temperature on the structure of water. *J. Phys. Chem.*, *72*(3), 899–905.

Bounaaj, A. (1990). *Modification structurale de l'eau liquide par des substances ioniques, organiques et biologiques. Etude par effet Raman*. Doctoral thesis, Université de Montpellier.

Bratos, S., & Tarjus, G. (1980). Optical methods of investigating molecular dynamics of liquids. In *Physics of modern materials* (pp. 571–577). Vienna: International Atomic Energy Agency.

Brooker, M. H., Hancock, G., Rice, B. C., & Shapter, J. (1989). Raman frequency and intensity studies of liquid $H_2O.H_2$,18)O and D_2O. *J. Raman Spectrosc.*, *20*(10), 683–694.

Burke, L. A., Jensen, J. O., Jensen, J. L., & Krishnan, P. N. (1993). Theoretical study of water clusters. I. Pentamer. *Chemical Physics Letters*, *206*(1-4), 293–296.

Busing, W. R., & Hornig, D. F. (1961). The effect of dissolved KBr, KOH or HCl on the Raman spectrum of water. *J. Phys. Chem.*, *65*(2), 284–292.

Carey, D. M., & Korenowski, G. M. (1998). Measurement of the Raman spectrum of liquid water. *J. Chem. Phys.*, *108*(7), 2669–2675.

Chaplin, M. F. (1999). A proposal for the structuring of water. *Biophysical Chemistry*, *83*(3), 211–221.

Chatzidimitriou-Dreismann, C. A., Krieger, U. K., Moeller, A., & Stern, M. (1995). Evidence of quantum correlation effects of protons and deuterons in the Raman spectra of liquid H_2O-D_2O. *Phys. Rev. Lett.*, *75*(16), 3008–3011.

Colles, M. J., Walrafen, G. E., & Wecht, K. W. (1970). Stimulated Raman spectra from H_2O, D_2O, HDO, and solutions of $NaClO_4$ in H_2O and D_2O. *Chemical Physics Letters*, *4*(10), 621–624.

Cross, P. C., Burnham, J., & Leighton, P. A. (1937). The Raman spectrum and the structure of water. *J. Amer. Chem. Soc.*, *59*(6), 1134–1147.

Cunningham, K., & Lyons, P. A. (1973). Depolarization ratio studies on liquid water. *J. Chem. Phys.*, *59*(4), 2132–2139.

D'Arrigo, G., Maisano, G., Mallamace, F., Migliardo, P., & Wanderlingh, F. (1981). Raman scattering and structure of normal and supercooled water. *J. Chem. Phys.*, *75*(9), 4264–4270.

Dorsey, N. E. (1940). *Properties of ordinary water—substance in all its phases: water-vapor, water, and all the ices*. Washington, DC: National Bureau of Standards.

Dougherty, R. C., & Howard, L. N. (1998). Equilibrium structural model of liquid water: evidence from heat capacity, spectra, density, and other properties. *J. Chem. Phys.*, *109*(17), 7379–7393.

Durig, J. R., Gounev, T. K., Nashed, Y., Ravindranath, K., Srinivas, M., & Rao, N. R. (1999). On the Raman spectra of liquid water as a function of temperature. *Asian J. Spectrosc.*, *3*(4), 145–154.

Dyke, T. R., Mack, K. M., & Muenter, J. S. (1977). The structure of water dimer from molecular beam electric resonance spectroscopy. *J. Chem. Phys.*, *66*(2), 498–510.

Easteal, A. J., Vernon, A., Edge, J., & Wolf, L. A. (1984). Isotope effects in water. Tracer diffusion coefficients for $H_2^{18}O$ in ordinary water. *J. Phys. Chem.*, *88*(24), 6060–6063.

Eckardt, G., & Wagner, W. G. (1966). On the calculation of absolute Raman scattering cross sections from Raman scattering coefficients. *J. Mol. Spectrosc.*, *19*(4), 407–411.

Eucken, A. (1946). Zur Kenntnis der Konstitution des Wassers. *Nachr. Ges. Wiss. Göttingen, Math.-physik. Klasse*, *1*, 38–48.

Eucken, A. (1949). Weiters zur Assoziation des Wassers. *Z. Elektrochem*, *53*(3), 102–105.

Foresman, J. B., & Frisch, Æ. (1996). *Exploring chemistry with electronic structure methods* (2nd ed.). Pittsburgh: Gaussian.

Frank, H. S., & Quist, A. S. (1961). Pauling's model and the thermodynamic properties of water. *J. Chem. Phys.*, *34*(2), 604–611.

Frank, H. S., & Wen, W. Y. (1957). Structural aspects of ion-solvent interaction in aqueous solutions: a suggested picture of water structure. *Disc. Faraday Soc.*, *24*, 133–140.

Frantz, J. D., Dubessy, J., & Mysen, B. (1993). An optical cell for Raman spectroscopic studies of supercritical fluids and its application to the study of water to 500 °C and 2000 bar. *Chemical Geology*, *106*(1–2), 9–26.

Frisch, M. J., Yamaguchi, Y., Gaw, J. F., & Schaefer, H. F. III (1986). Analytic Raman intensities from molecular electronic wave functions. *J. Chem. Phys.*, *84*(1), 531–532.

Giguere, P. A., & Chen, H. (1984). Hydrogen bonding in hydrogen peroxide and water. A Raman study of the liquid state. *J. Raman Spectrosc*, *15*(3), 199–204.

Giguere, P. A., & Pigeon-Gosselin, M. (1986). The nature of the ''free'' OH groups in water. *J. Raman Spectrosc.*, *17*(4), 341–344.

Green, J. L., Lacey, A. R., & Sceats, M. G. (1986). Spectroscopic evidence for spatial correlations of hydrogen bonds in liquid water. *J. Phys. Chem.*, *90*(17), 3958–3964.

Hagler, A. T., Scheraga, H. A., & Némethy, G. (1972). Structure of liquid water. Statistical thermodynamic theory. *J. Phys. Chem.*, *76*(22), 3229–3243.

Hare, D. E., & Sorensen, C. M. (1990). Raman spectroscopic study of bulk water supercooled to −33 °C. *J. Chem. Phys.*, *93*(1), 25–33.

Harvey, A. H., Gallagher, J. S., & Levelt Sengers, J. M. H. (1998). : Revised formulation for the refractive index of water and steam as a function of wavelength, temperature and density. *J. Phys. Ref. Chem. Data*, *27*(4), 761–774.

Hawlicka, E., & Grabowski, R. (1992). Self-diffusion in water-alcohol systems. 3. 1-propanol-water solutions of NaI. *J. Phys. Chem.*, *96*(4), 1554–1557.

Honegger, E., & Leutwyler, S. (1988). Intramolecular vibrations of small water clusters. *J. Chem. Phys.*, *88*(4), 2582–2595.

Hornung, N. J., Choppin, G. R., & Renovitch, G. (1974). The structure of water and its solutions. *Applied Spectroscopy Rev.*, *8*(2), 149–181.

Hutteau, F. (1998). *Contribution à l'étude physico-chimique du mécanisme de la saveur sucrée*. Doctoral thesis, Université de Reims Champagne-Ardenne.

Jensen, J. O., Krishnan, P. N., & Burke, L. A. (1995a). Theoretical study of water clusters: heptamers. *Chemical Physics Letters*, *241*(3), 253–260.

Jensen, J. O., Krishnan, P. N., & Burke, L. A. (1995b). Theoretical study of water clusters: octamer. *Chemical Physics Letters*, *246*(1-2), 13–19.

Jensen, J. O., Krishnan, P. N., & Burke, L. A. (1996). Theoretical study of water clusters: nonamers. *Chemical Physics Letters*, *260*(3-4), 499–506.

Jhon, M. S., Grosh, J., Ree, T., & Eyring, H. (1966). Significant structure theory applied to water and heavy water. *J. Chem. Phys.*, *44*(4), 1465–1472.

Johnson, K. (2000). ''Water buckyballs''–chemical, catalytic, and cosmic implications. *Infinite Energy*, *6*(33), 29–32.

Kęcki, Z., Witanowski, J., Akst-Lipszyc, K., & Minc, S. (1966). Mutual interactions in solutions of polar substances as observed in the Raman effect. Part X. Effect of electrolytes on water. *Roczniki Chem.*, *40*, 919–929.

Kim, J., & Kim, K. S. (1998). Structures, binding energies, and spectra of isoenergetic water hexamer clusters: extensive ab initio studies. *J. Chem. Phys.*, *109*(14), 5886–5895.

Kim, J., Lee, J. Y., Lee, S., Mhin, B. J., & Kim, K. S. (1995). Harmonic vibrational frequencies of the water monomer and dimer: comparison of various levels of ab initio theory. *J. Chem. Phys.*, *102*(1), 310–317.

Kim, J., Majumdar, D., Lee, H. M., & Kim, K. S. (1999). Structures and energetics of the water heptamer: comparison with the water hexamer and octamer. *J. Chem. Phys.*, *110*(18), 9128–9134.

Kim, K. S., Mhin, B. J., Choi, U., & Lee, K. (1992). Ab initio studies of the water dimer using large basis sets: The structure and thermodynamic energies. *J. Chem. Phys.*, *97*(9), 6649–6662.

Kint, S., & Scherer, J. R. (1978). : Intermolecular coupling in liquid water. *J. Chem. Phys.*, *69*(4), 1429–1431.

Knochenmuss, R., & Leutwyler, S. (1992). Structures and vibrational spectra of water clusters in the self-consistent approximation. *J. Chem. Phys.*, *96*(7), 5233–5244.

Kohl, W., Lindner, H. A., & Franck, E. U. (1991). Raman spectra of water to 400 °C and 3000 bar. *Ber. Bunsenges. Phys. Chem.*, *95*(12), 1586–1593.

Krishnan, P. N., Jensen, J. O., & Burke, L. A. (1994). Theoretical study of water clusters. II. Hexamer. *Chemical Physics Letters*, *217*(3), 311–318.

Lentz, B. R., Hagler, A. T., & Scheraga, H. A. (1974). Structure of liquid water. II. Improved statistical thermo-dynamic treatment and implications of a cluster model. *J. Phys. Chem.*, *78*(15), 1531–1550.

Libnau, F. O., Toft, J., Christy, A. A., & Kvalheim, O. M. (1994). Structure of liquid water determined from infrared temperature profiling and evolutionary curve resolution. *J. Am. Chem. Soc.*, *116*(18), 8311–8316.

Lindner, H.A. (1970). *Raman spektroskopische untersuchungen an HDO und H_2O bis 400 °C und 5000 bar*. Doctoral thesis, University of Karlsruhe.

Liu, K., Brown, M. G., Carter, C., Saykally, R. J., Gregory, J. K., & Clary, D. C. (1996a). Characterization of a cage form of the water hexamer. *Nature*, *381*(6582), 501–503.

Liu, K., Cruzan, J. D., & Saykally, R. J. (1996b). Water clusters. *Science*, *271*(5251), 929–933.

Long, D. A. (1977). *Raman spectroscopy*. New York: McGraw-Hill.

Luck, W. A. P. (1976). Water in biological systems. *Topics Curr. Chem.*, *64*(Inorganic Biochemistry), 113–180.

Luu, D. V., Cambon, L., & Mathlouthi, M. (1990). Perturbation of liquid-water structure by ionic substances. *J. Mol. Struct.*, *237*, 411–419.

Luu, C., Luu, D. V., & Boiron, J. (1980). Perturbation de la structure de l'eau liquide par effet thermique et par la présence d'une substance étrangére. I—effect thermique. *Trav. Soc. Pharm. Montpellier*, *40*(1), 41–54.

Luu, C., Luu, D. V., Rull, F., & Sopron, F. (1982). Etude par effet Raman de la perturbation structurale de l'eau liquide par une substance etrangere. Partie I. Modele d'association de l'eau liquide. *J. Mol. Struct.*, *81*(1-2), 1–10.

Moskovits, M., & Michaelian, K. H. (1978). A reinvestigation of the Raman spectrum of water. *J. Chem. Phys.*, *69*(6), 2306–2311.

Murphy, W. F., & Bernstein, H. J. (1972). Raman spectra and an assignment of the vibrational stretching region of water. *J. Phys. Chem.*, *76*(8), 1147–1152.

Narten, A. H., Danford, M. D., & Levy, H. A. (1967). X-ray diffraction study of liquid water in the temperature range 4-200 °C. *Disc. Faraday Soc.*, *43*, 97–107.

Némethy, G. (1974). Recent structural models for liquid water. In W. A. P. Luck (Ed.), *Structure of water and aqueous solutions* (pp. 73–91). Weinheim: Verlag Chemie.

Némethy, G., & Scheraga, H. A. (1962). Structure of water and hydrophobic bonding in proteins. I. A model for the thermodynamic properties of liquid water. *J. Chem. Phys.*, *36*(12), 3382–3400.

Pimentel, G. C., & McClellan, A. L. (1960). *The hydrogen bond*. New York: Reinhold Publ.

Pople, J. A. (1951). Molecular association in liquids. II. A theory of the structure of water. *Proc. Roy. Soc. (London)*, *A205*(1081), 163–178.

Prigogine, I., & Defay, R. (1954). *Chemical thermodynamics*. London: Longmans Green & Co.

Quine, B. M., & Drummond, J. R. (2002). GENSPECT: A line-by-line code with selectable interpolation error tolerance. *J. Quant. Spectrosc. Radiat. Transfer.*, *74*(2), 147–165.

Quintana, I. M., Ortiz, W., & López, G. E. (1998). Determination of the structure and stability of water clusters using temperature dependent techniques. *Chemical Physics Letters*, *287*(3-4), 429–434.

Rahman, A., & Stillinger, F. H. (1971). Molecular dynamics study of liquid water. *J. Chem. Phys.*, *55*(7), 3336–3359.

Rao, I. R. (1931). The behaviour of water with change of temperature and with addition of electrolytes as studied by the Raman effect. *Proc. Roy. Soc. (London)*, *A130*(814), 489–499.

Rao, I. R. (1934). The constitution of water in different states. *Proc. Roy. Soc. (London)*, *A145*(855), 489–508.

Rao, N. R., & Ramanaiah, K. V. (1966). Depolarization study of the components of the Raman band of water: evaluation of the relative abundance of the $(H_2O)_5$ and H_2O species. *Indian J. Pure & Appl. Phys.*, *4*(3), 105–108.

Ratcliffe, C. I., & Irish, D. E. (1982). Vibrational spectral studies of solutions at elevated temperatures and pressures. 5. Raman studies of liquid water up to 300 °C. *J. Phys. Chem.*, *86*(25), 4897–4905.

Röntgen, W. K. (1892). Über die Konstitution des flüssigen Wassers. *Ann. Physik*, *45*, 91–97.

Sceats, M., Rice, S. A., & Butler, J. E. (1975). The stimulated Raman spectrum of water and its relationship to liquid structure. *J. Chem. Phys.*, *63*(12), 5390–5400.

Sceats, M. G., Stavola, M., & Rice, S. A. (1979). A zeroth order random network model of liquid water. *J. Chem. Phys.*, *70*(8), 3927–3938.

Scherer, J. R. (1978). The vibrational spectroscopy of water. In J. H. Clark, & R. E. Hester (Eds.), *Advances in infrared and raman spectroscopy,* vol. 5 (pp. 149–216). London: Heyden.

Scherer, J. R., Go, M. K., & Kint, S. (1973). Raman spectra and structure of water in dimethyl sulfoxide. *J. Phys. Chem.*, *77*(17), 2108–2117.

Scherer, J. R., Go, M. K., & Kint, S. (1974). Raman spectra and structure of water from −10 to 90 °C. *J. Phys. Chem.*, *78*(13), 1304–1313.

Scherer, J. R., Kint, S., & Bailey, G. F. (1971). Spectral display of isotropic and anisotropic Raman scattering. *J. Mol. Spectrosc.*, *39*(1), 146–148.

Schultz, J. W., & Hornig, D. F. (1961). The effect of dissolved alkali halides on the Raman spectrum of water. *J. Phys. Chem.*, *65*(12), 2131–2138.

Serghat, S. (1993). *Contribution a l'etude physico-chimique de la perception de la saveur sucree: role de la structure de l'eau.* Doctoral thesis, Université de Reims Champagne-Ardenne.

Seuvre, A.-M. (1989). *Contribution à l'étude des interactions solvant-solute en solutions aqueuses de sucres et de sels*. Doctoral thesis, Université de Rouen.

Sokolowska, A. (1989). Effect of temperature on the Fermi resonance and the resonance intermolecular coupling in the Raman spectra of liquid water. *J. Raman Spectrosc.*, *20*(12), 779–783.

Speedy, R. J., Madura, J. D., & Jorgensen, W. L. (1987). Network topology in simulated water. *J. Phys. Chem.*, *91*(4), 909–913.

Stevenson, D. P. (1965). On the monomer concentration in liquid water. *J. Phys. Chem.*, *69*(7), 2145–2152.

Sutherland, W. (1900). The molecular constitution of water. *Phil. Mag.*, *50*, 460–489.

Symons, M. C. R. (1972). The structure of liquid water. *Nature*, *239*(5370), 257–259.

Szymanski, H. A. (1967). *Raman spectroscopy. Theory and practice*. New York: Plenum Press.

Wales, D. J., & Hodges, M. P. (1998). Global minima of water clusters $(H_2O)_n$, $n \leqslant 21$, described by an empirical potential. *Chemical Physics Letters*, *286*(1-2), 65–72 (also visit the Cambridge Cluster Database at: http//:www.wales.ch.cam.ac.uk/~wales/CCD/TIP4P-water.html).

Walrafen, G. E. (1964). Raman spectral studies of water structure. *J. Chem. Phys.*, *40*(11), 3249–3256.

Walrafen, G. E. (1967). Raman spectral studies of the effects of temperature on water structure. *J. Chem. Phys.*, *47*(1), 114–126.

Walrafen, G. E. (1970). Raman spectral studies of the effects of perchlorate ion on water structure. *J. Chem. Phys.*, *52*(8), 4176–4198.

Walrafen, G. E. (1974). Spontaneous and stimulated Raman spectra from water and aqueous solutions. In W. Luck (Ed.), *Structure of water and aqueous solutions* (pp. 301–321). Weinheim: Verlag Chemie.

Walrafen, G. E., Fisher, M. R., Hokmabadi, M. S., & Yang, W.-H. (1986a). Temperature dependence of the low- and high-frequency Raman scattering from liquid water. *J. Chem. Phys.*, *85*(12), 6970–6982.

Walrafen, G. E., Hokmabadi, M. S., & Yang, W.-H. (1986b). Raman isobestic points from liquid water. *J. Chem. Phys.*, *85*(12), 6964–6969.

Weston, R. E. (1962). Raman spectra of electrolyte solutions in light and heavy water. *Spectrochim. Acta*, *18*(9), 1257–1277.

Wicke, E. (1966). Structure formation and molecular mobility in water and in aqueous solutions. *Angewandte Chemie (Intl. Ed.)*, *5*(1), 106–122.

Xantheas, S. S., & Dunning, T. H. (1993). Ab initio studies of cyclic water clusters $(H_2O)_n$, $n = 1$-6. I. Optimal structures and vibrational spectra. *J. Chem. Phys.*, *99*(11), 8774–8792.

Xantheas, S. S. (1994). Ab initio studies of cyclic water clusters $(H_2O)_n$, $n = 1$-6. II. Analysis of many-body interactions. *J. Chem. Phys.*, *100*(10), 7523–7534.

Xantheas, S. S. (1995). Ab initio studies of cyclic water clusters $(H_2O)_n$, $n = 1$-6. III. Comparison of density functional with MP2 results. *J. Chem. Phys.*, *102*(11), 4505–4517.

Yeh, Y., Bilgram, J. H., & Känzig, W. (1982). Raman spectra of supercooled H_2O from 0 to−21 °C. *J. Chem. Phys.*, *77*(5), 2317–2321.

Zhelyaskov, V., Georgiev, G., & Nikolov, Z. (1988). Temperature study of intra- and intermolecular coupling and Fermi resonance constants in the Raman spectra of liquid water using Fourier deconvolution. *J. Raman Spectrosc.*, *19*(6), 405–412.